USGS
science for a changing world

Cenozoic Distributed Volcanism of the Arabia Plate—A Review

Chapter J of
Distributed Volcanism—Characteristics, Processes, and Hazards

Professional Paper 1890

U.S. Department of the Interior
U.S. Geological Survey

Cover. View southeast across trachyte crater of Gura 3, northern Ŧarrat Rahat. Note camels in small foreground sabkha (mudflat). U.S. Geological Survey photograph by A.T. Calvert, February 16, 2014.

Cenozoic Distributed Volcanism of the Arabia Plate—A Review

By Thomas W. Sisson and Andrew T. Calvert

Chapter J of
Distributed Volcanism—Characteristics, Processes, and Hazards
Edited by Michael P. Poland, Michael H. Ort, Wendy K. Stovall, R. Greg Vaughan, Charles B. Connor, and M. Elise Rumpf

Professional Paper 1890

U.S. Department of the Interior
U.S. Geological Survey

U.S. Geological Survey, Reston, Virginia: 2026

Suggested citation:
Sisson, T.W., and Calvert, A.T., 2026, Cenozoic distributed volcanism of the Arabia Plate—A review, chap. J *of* Poland, M.P., Ort, M.H., Stovall, W.K., Vaughan, R.G., Connor, C.B., and Rumpf, M.E., eds., Distributed volcanism—Characteristics, processes, and hazards: U.S. Geological Survey Professional Paper 1890, 28 p., https://doi.org/10.3133/pp1890J.

ISSN 2330-7102 (online)

Acknowledgments

This report relies heavily on discoveries made by participants in a joint Saudi Geological Survey (SGS) and U.S. Geological Survey (USGS) effort studying volcanism and volcanic and seismic hazards of northern Ḩarrat Rahat, Kingdom of Saudi Arabia. These include, but are not limited to, for the SGS: Hani Zahran, Jamal Shawali, Khalid Hassan Hafez, Salah El-Hadidy Youssef, Adel Shareef, Maher Al-Dahri, Mahmoud Ashour, Mahmoud Sami, Wael Alraddadi, Talal Alsammery, Vladimir Sokolov, Ian C.F. Stewart, and John Roobol, all under the leadership of Dr. Zohair A. Nawab, SGS President (retired); and for the USGS: Paul Bedrosian, Alex Blanchette, Duane Champion, Hannah Dietterich, Drew Downs, Victoria Langenheim, Gail Mahood, Walter Mooney, Timothy Orr, Jared Peacock, Joel Robinson, Juliet Ryan-Davis, Vincent J.M. Salters, David Sherrod, and Mark Stelten. Additional guidance was provided by Professors M. Rashad Moufti and Talal A. Mokhtar, King Abdulazziz University; Simon Klemperer, Stanford University; and by Peter Johnson, SGS retired; Ryota Kiuchi, Kyoto University (now at Kozo Keikaku Engineering); Francesco Civilini, California Institute of Technology (now at National Aeronautics and Space Administration Goddard); and Zhixiang Yao, Institute of Geophysics, China Earthquake Administration. Staff of the U.S. Consulate, Jiddah, facilitated entry and exit from the Kingdom of Saudi Arabia. Constructive reviews by Vic Camp and Marco Brenna are gratefully acknowledged.

Contents

Figures

Conversion Factors

International System of Units to U.S. customary units

Multiply	By	To obtain
	Length	
meter (m)	3.281	foot (ft)
kilometer (km)	0.6214	mile (mi)
	Area	
square kilometer (km^2)	0.3861	square mile (mi^2)
	Volume	
cubic kilometer (km^3)	0.2399	cubic mile (mi^3)
	Speed	
meter per second (m/s)	3.281	foot per second (ft/s)
kilometer per second (km/s)	0.6214	mile per second (mi/s)
	Pressure	
Gigapascal (GPa)	9869.2	atmosphere, standard (atm)

Temperature in degrees Celsius (°C) may be converted to degrees Fahrenheit (°F) as °F = (1.8 × °C) + 32.

Abbreviations

CIPW norm	rock chemical compositions recast into weight percent of rock-forming minerals by the method of Cross, Iddings, Pirsson, and Washington
GPa	gigapascals (10^9 pascals) pressure
ka	kilo-annum (thousand years ago)
k.y.	thousand years duration
Ma	Mega-annum (million years ago)
Mg#	Mg number (=100×Mg/[Mg+Fe^{2+}], molar)
MMN line	Makkah-Madīnah-Nafud line
MORB	midocean ridge basalts
SGS	Saudi Geological Survey
USGS	U.S. Geological Survey
VORiSA	Volcanic Risks in Saudi Arabia Project

Distributed Volcanism—Characteristics, Processes, and Hazards
Edited by Poland, Ort, Stovall, Vaughan, Connor, and Rumpf
Professional Paper 1890

Chapter J

Cenozoic Distributed Volcanism of the Arabia Plate—A Review

By Thomas W. Sisson and Andrew T. Calvert

Abstract

Cenozoic volcanic rocks of the Arabia Plate cover about 140,000 square kilometers across a distance of about 3,000 kilometers from southern Yemen to southeastern Turkey. The majority of volcanic products are alkali basalts that erupted in restricted areas, commonly over periods of a million or more years, building mafic lava fields, each known in Arabic as a "harrat." Harrat volcanism commenced following the Oligocene flood-lava effusions that blanketed the (now) Ethiopian highlands, southern Sudan, and western Yemen, and overlapped the latest Oligocene to early Miocene initial riftings of the Red Sea and Gulf of Aden, but the majority of harrat volcanism has been since approximately 13–10 million years ago. Persistent harrat magmatism in restricted locations led to the development of intermediate and evolved magmas (hawaiites, mugearites, benmoreites, trachytes, comendites, and phonolites) mainly through intracrustal crystallization-differentiation. Most of these intermediate and evolved magmas erupt at sites of the greatest aggregate volcanic relief, reflecting sites of the greatest overall magmatic fluxes. Production of fractionated magmas at these sites negates "monogenetic" as an appropriate descriptor of harrat volcanism. This chapter summarizes the geologic, eruptive, and tectonic history and aspects of the petrogenesis of the Cenozoic Arabian alkalic province. Particular emphasis is placed on results of a joint study of Ḥarrat Rahat adjacent to the city of Al Madīnah al Munawwarah, Kingdom of Saudi Arabia, published as U.S. Geological Survey Professional Paper 1862 and Saudi Geological Survey Special Report SGS–SP–2021–1. A goal of this chapter is to provide an introduction to those unfamiliar with this vast, enigmatic, and fascinating region of distributed continental volcanism.

Introduction

The Arabian harrats[1] are Cenozoic volcanic fields, dominantly mafic and alkalic, scattered discontinuously north up the Arabian Peninsula from Yemen's south coast about 2,400 kilometers (km) to Damascus, Syria, or almost 3,000 km if the Karaca Dağ (also written Karacalidag) volcanic field, southern Turkey, is included (fig. 1). The latter distance is the same as from Santorini volcano, Greece, to the England-Scotland border, or from Yellowstone Lake, United States, to Mexico City, Mexico. As such, the Arabian harrat belt is one of Earth's major provinces of distributed continental volcanism. Similar in extent and overall setting are the late Mesozoic to Cenozoic alkalic volcanic fields of eastern Australia that span approximately (~) 3,800 km from northern Queensland to Tasmania (Ewart and others, 1988; Shea and others, 2022) and the Cenozoic alkalic lava fields of north-central Africa that stretch about 2,100 km from the Jabāl as Sawdā' volcanic field, central Libya, through the Tibesti mountains of northern Chad, to the Meidob, Kutum, and Jebēl Marra volcanic fields of western Sudan (Siebert and others, 2010). Members of the Arabian harrat province range from clusters of a few scoria cones with associated small lava flows to the 48,000 square kilometer (km^2) Ḥarrat ash Shamā of Syria, Jordan, and northwestern Saudi Arabia. Causes are enigmatic for intraplate volcanism across such great expanses. Plate extension with consequent lithospheric thinning and mantle decompression-melting could be indicated by the Arabian harrat belt's proximity to and sub-parallelism with the Red Sea, but although normal faults cut portions of the Arabian Shield and Platform, the faults are modest and few, lacking the prominence, abundance, and substantial offsets that appreciable crustal extension would create. Some association with the Afar mantle plume is evident, but difficult to explain is why plume-driven volcanism would extend 3,000 km as a belt across a continental plate, instead of being distributed more uniformly around the plume center, or why continental volcanism would persist in localized areas of the Arabia Plate for millions to tens of millions of years. The upwellings of depleted asthenosphere that feed the midocean ridge basalts (MORB) of the southern Red Sea and Gulf of Aden also must interrupt direct connections between the spreading Afar plume head and the base of the Arabia Plate. Similar uncertainties hold for the east Australian and north-central African intraplate volcanic provinces.

Harrat volcanism also does not fit comfortably into commonly used classifications of basaltic volcanoes and volcanic systems. The small scoria cone clusters readily meet expectations of monogenetic volcanism, but the harrats consist mostly of fields of overlapping lava flows that erupted intermittently from approximately linear vent arrays over periods of a million or more years in a particular area. Their persistent activity in focused areas is a defining characteristic not captured

[1]"Ḥarrat" is the Arabic possessive noun referring to a particular expansive region of dark, rubbly volcanic rocks; "harrah" or "harra" is the general or non-possessive noun.

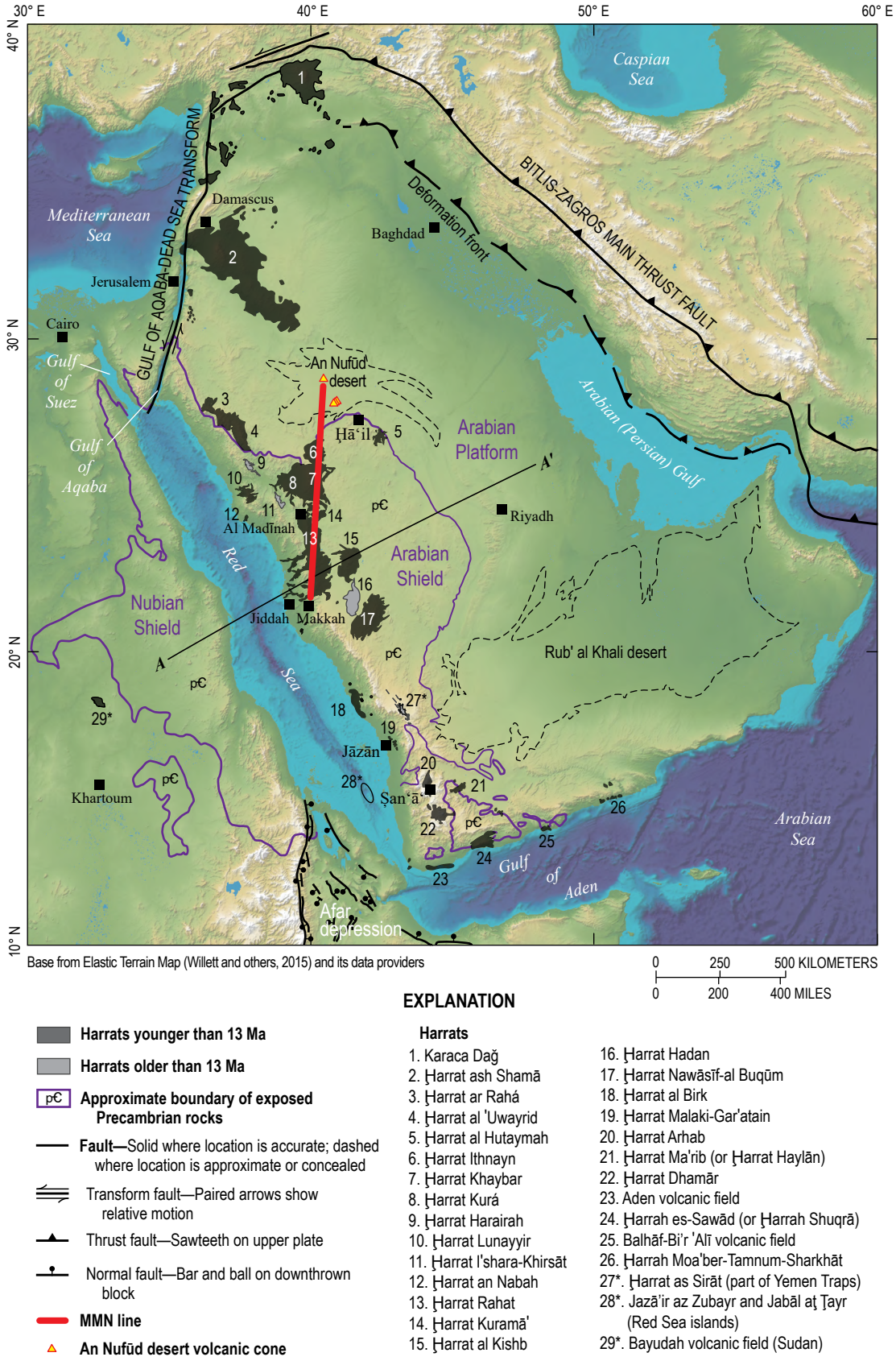

Figure 1. Colored shaded-relief map of the Arabian Peninsula and vicinity, showing the tectonic setting of subaerial Cenozoic mafic volcanic fields (harrats). Shown are harrats chiefly younger than 13 million years ago (Ma), as well as a smaller number of harrats older than 13 Ma; omitted are Oligocene basaltic traps, Neogene to Quaternary volcanic rocks of the Afar depression, and all submarine volcanic rocks. MMN line refers to the Makkah-Madīnah-Nafud volcanic axis of Camp and Roobol (1992). Asterisks indicate Cenozoic volcanic fields not on the Arabian Peninsula (no. 28 and 29) and an isolated erosional remnant of the Oligocene Yemen Traps referred to by residents and in the literature as a harrat (no. 27). Refer to figure 13 for topographic and geophysical cross section *A*–*A*'. Extents of Arabian and Nubian Shield rocks, plate-bounding structures, and faults modified from U.S. Geological Survey and Arabian American Oil Company (1963), Coleman and others (1983), Bosworth and others (2005), and Stern and Johnson (2010).

by the possibly monogenetic character of any particular vent or eruption. As will be shown, this prolonged spatial localization produces intermediate and evolved magmas that clearly are not monogenetic, among other consequences. Owing to their broad areas, the harrats have been described as medium-sized flood basalts (Walker, 1993), but they lack the volumes and brevities typical of flood eruptions. Their prolonged activity in particular locations shares aspects of central volcanoes, but in most cases their magma supply systems are insufficiently localized and sustained to have produced summit calderas. Their long-term growth by repeated eruptions along linear vent chains constructs elongated edifices that resemble, at least in landform, the rift zones of large shield volcanoes. However, evidence is absent, or has not been recognized, for appreciable along-rift transport of magma from a central location of supply, unlike the rift-zone eruptions familiar from Hawaiian shield volcanoes. Too repeatedly active and long-lived for monogenetic to be their meaningful descriptor, but insufficiently active to support the focused feeder systems of shield and central volcanoes, they are perhaps best characterized simply as sustained basaltic volcanic fields, and "harrats" might be adopted more widely as a general term for such volcanic systems.

This report's goal is to introduce and summarize the overall characteristics of the Cenozoic distributed volcanism of the Arabia Plate. Our familiarity with this area stems from a collaborative geologic and geophysical project between the Saudi Geological Survey (SGS) and the U.S. Geological Survey (USGS) studying the volcanic history and hazards of the northern portion of Ḥarrat Rahat adjacent to the city of Al Madīnah al Munawwarah (hereafter, Al Madīnah), Kingdom of Saudi Arabia. Results of that work are available as journal articles, cited where appropriate in this chapter, a geologic map (Downs and others, 2019; Robinson and Downs, 2023), and compiled in USGS Professional Paper 1862 (Sisson and others, 2023a, and chapters therein). Other key sources of information are geologic maps of some major harrats, with explanatory pamphlets, produced by Vic Camp and John Roobol, released through the SGS or its institutional predecessors (Camp and Roobol, 1991a; Roobol and Camp, 1991a,b) and associated interpretive journal articles (Camp and others, 1987, 1991, 1992; Camp and Roobol, 1989, 1991b, 1992). Also important are USGS summaries of harrat volcanism by Coleman and others (1983), Brown and others (1989), and Coleman (1993). The detailed volcanic geology of northern Ḥarrat Rahat was first investigated and interpreted by Moufti (1985), and all subsequent studies have adopted the names therein for places and most volcanic products. Moufti and Németh (2016) provide photographs, place names, and basic interpretations for noteworthy volcanic landforms in some Saudi Arabian harrats. Al-Onaizan and others (2017) list, name, and locate Saudi Arabian volcanic landforms exhaustively (in Arabic). A joint effort between King Abdulaziz University and the University of Auckland called the Volcanic Risks in Saudi Arabia (VORiSA) Project was carried out in 2011–2014 and focused principally on the physical volcanology of northern Ḥarrat Rahat and how this informs assessments of hazards (Lindsay and Moufti, 2014). Summaries of Cenozoic tectonics are presented by Bohannon and others (1989), Coleman (1993), Bosworth and others (2005), Bosworth (2015), and Reilinger and others (2015). Withstanding the test of time is Powers and others' (1966) authoritative description of the Arabian Platform sedimentary sequence. Stern and Johnson (2010) and Johnson and Kattan (2012) compiled and interpreted the geologic history of the Precambrian Arabian Shield.

Tectono-Magmatic Setting and History

Since the earliest conceptions of continental drift (Lartet, 1869; Wegener, 1915), the Red Sea, Gulf of Aden, and their flanking landmasses were recognized as the archetype of continental rifting, and the region has since figured prominently in developing and refining theories of plate tectonics (Baker, 1970; McKenzie and others, 1970; Burke and Dewey, 1973; Coleman 1974). Cenozoic tectonic events that influenced the region (fig. 1) included (1) collision of the Afro-Arabia Plate's northeastern continental margin against Eurasia thereby creating the Bitlis-Zagros suture as subduction consumed the last of the plate's leading oceanic edge and closed the Neotethys Ocean, (2) the Afar mantle plume impinging beneath the (now) Afar depression at the north end of the (now) East African Rift, (3) opening of the Red Sea and Gulf of Aden rifts separating the Arabia and Africa Plates, and (4) the Gulf of Aqaba-Dead Sea Transform fault system separating the Sinai block as the Arabia Plate continued to converge beneath Eurasia.

Associated volcanism on the continental portion of the Arabia Plate is divisible broadly into four stages, not wholly correlative with the aforementioned tectonic events: (1) eruptions of plume-impingement flood basalts around 30 million years ago (Ma) that blanketed what are now the Ethiopian highlands, southern Sudan, and western Yemen prior to the openings of the Red Sea, Gulf of Aden, and the Afar depression; (2) early harrat basaltic volcanism that immediately followed, forming a belt of centers scattered northward across the Arabia Plate as far as Ḥarrat ash Shamā (also known as Ḥarrat ash Shaam, Ḥarrat Shama, or Ḥarrat al Ḥarrah) in Syria, Jordan, and northwestern Saudi Arabia, or perhaps to Karaca Dağ volcanic field (Turkey); (3) regional tholeiitic basaltic diking in the period 24–20 Ma during initial Red Sea rifting, exposed mainly as rift-parallel dikes and small gabbroic intrusions on the Red Sea's subaerial eastern flank and as scattered basaltic volcanic fields including in the Cairo basin (Egypt) subsurface, with diminished volcanism continuing to about 15 Ma; and (4) dominantly mafic alkalic volcanism commencing around 13–12 Ma, and continuing to the present, that produced harrats and scattered smaller centers with well-preserved constructional volcanic relief and young-appearing volcanic landforms (Coleman and others, 1983; Bohannon, 1986; Bohannon and others, 1989; Camp and Roobol, 1989; Coleman, 1993; Ilani and others, 2001; Bosworth and others, 2005; Bosworth, 2015; Bosworth and Stockli, 2016). There may have been a hiatus, or nearly so, between the third and fourth stages (Ilani and others, 2001), but few efforts have been undertaken to date older harrat rocks, and their concealment beneath younger lavas hinders detailed studies and interpretations. Off-continent volcanism entailed Neogene and Quaternary submarine spreading-ridge and associated magmatism in the Red Sea and Gulf of Aden. This volcanism continues to the present and constructed the Arabia Plate's western and southern oceanic crustal margins locally

building the emergent and historically active volcanic islands of Jazā'ir az Zubayr and Jabāl aṭ Ṭayr in the southern Red Sea (fig. 1, no. 28).

Physiographic developments correlate with these tectono-magmatic phases. Most of the Arabian Shield now stands about 1,000 meters (m) above sea level but is covered unconformably to the north, east, and south by the gently outward-dipping Arabian Platform sedimentary sequence (fig. 1) that records marine passive-margin sedimentation spanning from the Cambrian, or perhaps latest Proterozoic, through the Neogene (Powers and others, 1966). Marine sedimentary rocks of this sequence crop out at elevations as great as 500 to 800 m above sea level, and in some areas as high as 1,200 m, indicating substantial post-depositional uplift but without short wavelength folding indicative of strong, localized compression, and, likewise, with few extensional faults; the shield appears to have uplifted en masse, or nearly so. Long-term development of the passive-margin sedimentary sequence is not relevant to this chapter, but a regional unconformity or disconformity high in the sequence places lower Miocene and younger clastic rocks atop upper Eocene marine carbonates (Powers and others, 1966; Swift and others, 1998). An unconformity at this level also cuts out most to all Oligocene strata in the Gulf of Suez and northern Red Sea, and this unconformity incises as deeply as Lower Cretaceous strata in the southern Red Sea (Bosworth, 2015). A late Oligocene plate-scale event of modest uplift and erosion, or non-deposition, followed by a regional change from carbonate to clastic sedimentation, accords with reconstructed plate motions indicating collision between the Afro-Arabian and Eurasian continental land masses commencing near the end of the Oligocene. This collision divided the Neotethys Ocean by early Miocene time (McQuarrie and others, 2003; Agard and others, 2011; McQuarrie and van Hinsbergen, 2013; Torsvik and Cocks, 2017).

Through improvements in dating, flood volcanism associated with the Afar mantle plume is now known to have taken place mainly in a brief pulse at 31–30 Ma, continuing sporadically to about 26.5 Ma, ending in some areas with voluminous eruptions of rhyolite (Bosworth and Stockli, 2016). In western Yemen, the flood basalts and succeeding rhyolites accumulated to thicknesses of 1–2.5 km and constitute about 10 percent of the ~600,000 km^2 area and greater than (>) 350,000 cubic kilometer (km^3) volume of the combined Ethiopia-Sudan-Yemen Traps (Baker and others, 1996; Menzies and others, 1997). Evidence around the Ethiopian highlands points to plume-impingement uplift perhaps commencing as much as 10 million years prior to flood volcanism (Sembroni and others, 2016; Faccenna and others, 2013, 2019), although interstratification of basal flood-lavas with shallow marine sedimentary rocks shows that some areas were near sea level at the onset of flood eruptions (Coleman, 1993). Most uplift associated with the Afar plume, however, followed emplacement of flood lavas (Menzies and others, 1997; Sembroni and others, 2016; Faccenna and others, 2013, 2019) and is apparent today as the high topography surrounding the Afar depression, including across the Red Sea in western Yemen and southwestern Saudi Arabia (fig. 1).

Much or all of the pre-rift Nubian-Arabian Shield was at elevations close to sea level in the Oligocene, as shown by marine mudstone and limestone intercalated with basal lavas of Ḥarrat Hadan (28–10 Ma) (Madden and others, 1980; Sebai and others, 1991) and lateritic paleosols or chert-pebble coquina exposed beneath basal lavas of other old harrats (Coleman, 1993). Lateritic paleosols and fossiliferous mudstones also underlie the flood basalts of the Yemen Traps, but $^{87}Sr/^{86}Sr$ isotopic values of fossils in those underlying rocks are unlike Oligocene seawater, suggesting lacustrine, rather than marine, paleoenvironments (Menzies and others, 1997). Geukens (1966) also identifies fossils in sedimentary strata within the Yemen Traps as fresh-water gastropods, lamellibranchs, and ostracods. The Red Sea rift basin had developed by the early Miocene into a distinctly bounded bathymetric low, as recorded by marine shales, sandstones, and carbonates that transgressed atop red beds. By the late Miocene, the basin was sufficiently deep and confined to accumulate great thicknesses of evaporitic salt (Coleman, 1993; Bosworth, 2015). Rift initiation along the Red Sea and Gulf of Aden appears to have been contemporaneous at 22±3 Ma, with the Red Sea initially opening orthogonal to the rift axis, but with the spreading rate approximately doubling at 11±2 Ma and the spreading direction becoming more north-northeasterly (Reilinger and others, 2015). This increase in spreading rate and change in spreading direction correspond, within uncertainty, with the onset of Gulf of Aqaba-Dead Sea Transform faulting and with the establishment of well-organized seafloor-spreading volcanism along the length of the Gulf of Aden (Bohannon and others, 1989; Reilinger and others, 2015; Szymanski and others, 2016). Rift-flank uplift near this time produced the Great Escarpment—the steep, west-facing mountain front along which the Ḥijāz highlands, from Makkah north to the Gulf of Aqaba, and the ʻAsīr highlands, to the south into Yemen, overlook the narrow Red Sea coastal plain (Tihāmat al Ḥijāz, Tihāmat ʻAsīr, and Tihāmat al Yemen). Harrat volcanism also became widespread and vigorous at about 12–10 Ma (Camp and Roobol, 1989; Coleman, 1993), with some large lava flows draping the Great Escarpment and reaching the Red Sea coastal plain, clearly showing that voluminous effusions continued after pronounced uplift (Camp and Roobol, 1989, 1991a; Ball and others, 2023). Extensional faults cut old harrats locally (Szymanski and others, 2016), but few such faults displace the younger harrats and only by small amounts; similarly, the Arabian Shield, although elevated, is low-relief and largely free of fault-bounded horst and graben topography, collectively indicating small-to-negligible amounts of crustal extension and thinning to the east of the Great Escarpment. The coincidence of events around and across the Arabia Plate at about the time of the middle to late Miocene transition is suggestive of a common cause for the diverse tectonic, geomorphic, and magmatic changes—perhaps widespread loss of the lower lithosphere of the Arabia Plate was focused beneath the shield and its capping belt of harrats (McGuire and Bohannon, 1989; Calvert and Sisson, 2023; Sisson and others, 2023b).

Harrat Distribution and Overall Character

The Saudi Arabian portion of the Cenozoic Arabian volcanic province is well characterized through the efforts and support of the SGS and its institutional predecessors. Measured from the axis of the Red Sea, Saudi Arabian harrats lie as close as 120–160 km (Ḥarrats an Nabah, Lunayyir, and al Birk) to as distant as 700 km (Ḥarrat al Hutaymah) (fig. 1). The younger harrats on the Arabian

Shield can be divided into a narrow, central, more active zone consisting, from south to north, of Ḫarrats Rahat, Khaybar, and Ithnayn that are large and have substantial constructional volcanic relief (300–600 m), flanked to the west and east by smaller, less active harrats. Camp and Roobol (1992) recognized and named this central active belt the Makkah-Madīnah-Nafud line (MMN line), including Nafud in the name because of a volcanic cone known as Al ʻUlaym that emerges from the central An Nufūd erg (desert dune field) as well as volcanic cones that breach the sands near the village of Jubbah, close to the erg's southern margin (fig. 1). Tracing harrat crests, the MMN line is about 580 km long from southern Ḫarrat Rahat to northern Ḫarrat Ithnayn, or 780 km if extended to the Al ʻUlaym cone, with the zone of venting being 25–50 km broad within the constituent MMN line harrats. The MMN line has an overall north-south trend such that its crest lies closer to the Red Sea in the south and more distant in the north. The crest of the MMN line is about 240 km east of the Red Sea axis at southern Ḫarrat Rahat, 500 km east at Ḫarrat Ithnayn, and the al ʻUlaym cone lies 630 km east-northeast of the junction of the Red Sea axis with the Gulf of Aqaba-Dead Sea Transform fault system. The Paleozoic through Cenozoic Arabian Platform sedimentary sequence is arched into a broad, shallowly north-plunging antiform near the city of Ḥāʻil (fig. 1). Uplift along this Ḥāʻil arch is recorded as early as the Mesozoic Era by facies changes in Cretaceous rocks (Powers and others, 1966), and although some publications have equated the MMN line with the Ḥāʻil arch, the north end of the MMN line lies about 200 km west of the Ḥāʻil arch crest.

Alkali basalts are the dominant products of both MMN line harrats and the smaller harrats to its flanks, but the flanking harrats range to more alkaline compositions, with basanites being common and including phonolites as rare, highly evolved rock types, whereas evolved members of the MMN line are trachytes or rare comendites (fig. 2). Camp and Roobol (1992) further show

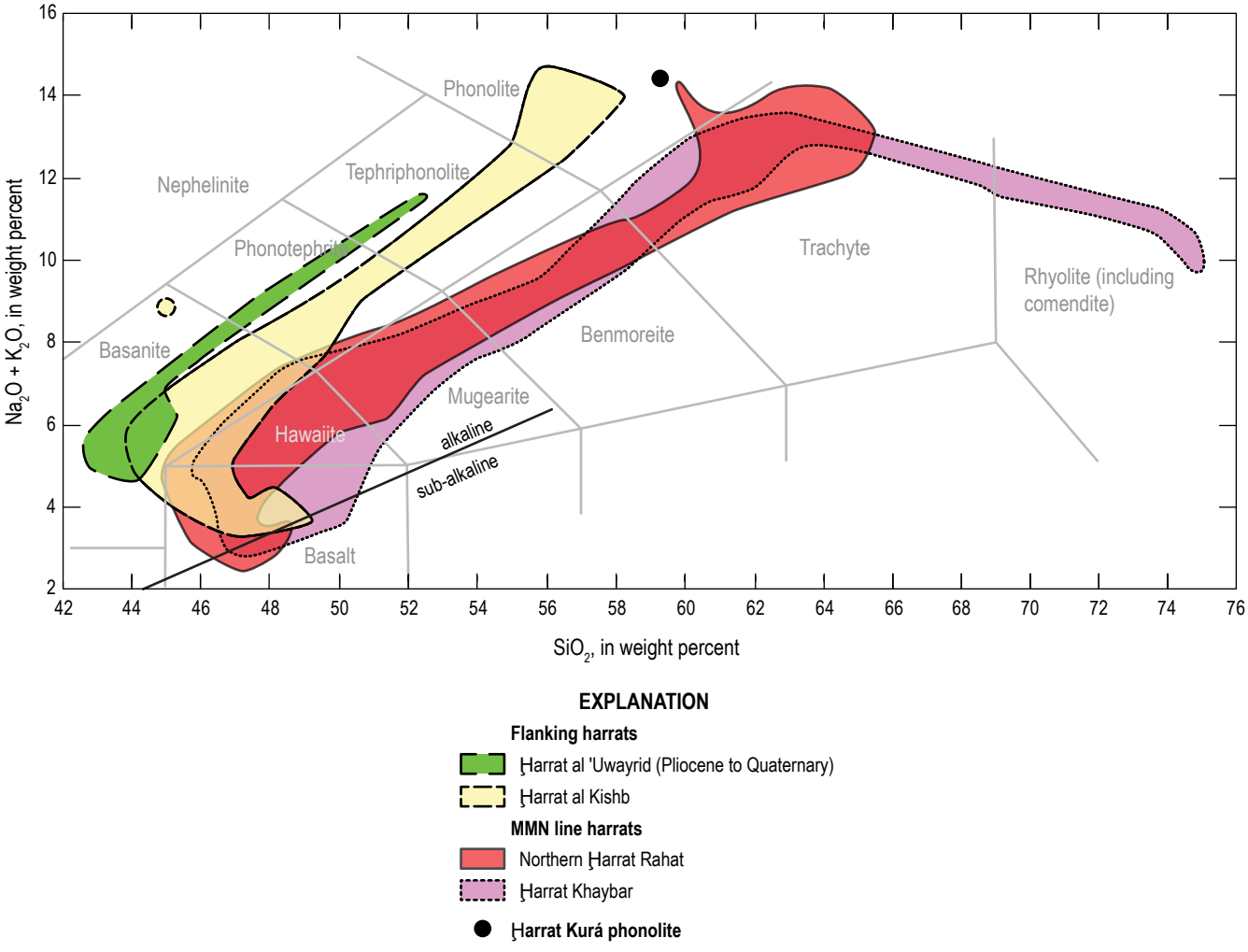

Figure 2. Total alkali-silica (TAS) diagram of concentrations of alkalis (Na_2O+K_2O) versus silica (SiO_2), in weight percent, showing fields for volcanic rocks from representative Makkah-Madīnah-Nafud line (MMN line) harrats and from representative harrats flanking to the west and east. MMN line harrats are volcanic rocks from northern Ḫarrat Rahat (Downs, 2019; Brenna and others, 2019) and Ḫarrat Khaybar (Camp and others, 1991; Roobol and Camp, 1991a). Representative flanking harrats are Ḫarrat al Kishb (Camp and others, 1992) and the Pliocene to Quaternary volcanic rocks of Ḫarrat al ʻUwayrid (Altherr and others, 2019). The black circle shows phonolite from Ḫarrat Kurá, older than and just west of Ḫarrat Khaybar (Camp and others, 1991). Gray lines delimit the volcanic rock classification fields of Le Bas and Streckeisen (1991). The inclined straight black line separates alkaline from subalkaline volcanic rocks after MacDonald and Katsura (1964).

that lavas from flanking harrats reach higher Nb/Zr compositions than do lavas of the MMN line; this and their more alkalic character indicate that flanking-harrat magmas form by lesser extents of partial melting than for magmas that feed the MMN line. Peridotite xenoliths are also widespread in the flanking harrats but are nearly absent along the MMN line, the exception being peridotite nodules reported for Ḥarrat Ithnayn (Coleman and others, 1983; Camp and others, 1991). Collectively, these observations point to a zone of enhanced partial melting centered beneath the MMN line and lower extents of melting to its flanks that extend across breadths of hundreds of kilometers. The magmatic fluxes feeding the MMN line harrats are also sufficient to have created crustal intrusive complexes where parental basalts stall and differentiate to benmoreites, trachytes, or even comendites, thereby hindering mantle xenoliths from being carried to the surface. In contrast, many of the magmas of the flanking harrats must have ascended directly from mantle depths to have retained their cargoes of peridotite xenoliths.

Regarding classification, nearly all volcanic rocks of northern Ḥarrat Rahat have CIPW normative[2] nepheline if the samples' ferric and ferrous iron concentrations are calculated as appropriate for magmatic liquids at the fayalite-quartz-magnetite oxygen buffer (Sisson and others, 2023b). Rocks referred to in pre-2023 Ḥarrat Rahat publications as subalkaline "olivine transitional basalts" and even some "tholeiites" are therefore actually weakly alkaline, consistent with their lack of groundmass pigeonite or hypersthene. The alkaline-subalkaline discrimination of MacDonald and Katsura (1964) correctly distinguishes nepheline- versus hypersthene-normative samples, whereas that of Irvine and Baragar (1971) misclassifies many harrat basalts as subalkaline.

Notable is the asymmetry between the western Nubian and eastern Arabian sides of the Red Sea. Although incised Tertiary volcanic plugs and shallowly exhumed Tertiary dikes are scattered along the west (Nubian) side of the Red Sea, they are few and small, and the only harrat on that flank sufficiently young to preserve undissected cones and lava flow margins, excluding those in the Afar depression, is the Bayudah volcanic field in northern Sudan (fig. 1, no. 29). The Nubian Shield and its surroundings also stand about 500 m above sea level, contrasting with the ~1,000 m elevation of the Arabian Shield (Bohannon and others, 1989).

Considered in greater detail, the larger Arabian harrats are composites of smaller sub-harrats, each defined by a high-standing, elongate vent axis that in most cases is oriented and aligned approximately in series with those of its neighboring sub-harrats, but in other cases the elongate vent axes are offset laterally from one another. Ḥarrat Rahat consists of the former, being the coalesced product of four sub-harrats collectively aligned approximately north-south with the raised vent axis of each sub-harrat being 60–65 km in length and also oriented north-south to slightly west of north (fig. 3). Ḥarrat ash Shamā, the largest harrat by area, has five well-defined raised-vent areas, each elongate in a north-northwest to south-southeast direction, as well as more diffuse venting in its southeast end. The three raised vent loci on the east side of this harrat are aligned in a chain, as with Ḥarrat Rahat, but two vent loci at the north end of Ḥarrat ash Shamā are offset laterally to the west, overlapping along their lengths with those to the east (fig. 4).

Upper crustal structure influences the vent loci. Northern Ḥarrat Rahat's topographically high main vent axis lies on the harrat's east side with lower elevation vents scattered diffusely to the west forming a poorly defined western vent axis. Inversion of combined gravity and geomagnetics is consistent with northern Ḥarrat Rahat overlying a shallow, north-northwest striking half graben with the main, eastern vent axis situated above the down-to-the-west fault that defines the graben's east side (Langenheim and others, 2019, 2023). Additional north-northwest to south-southeast striking faults or fissures are indicated by similarly aligned vents to the west of the main vent axis, but detailed geologic mapping revealed only one normal fault and one open fissure system cutting the surface of the harrat within the area of the main vent axis (Downs and others, 2019; Robinson and Downs, 2023). Likewise, no faults or offsets were found displacing young sediments of nearby alluvial systems and sabkahs, so active tectonism appears minimal in the immediate area of the harrat. This contrasts with Miocene alkalic lavas that cap mesas to the west of Ḥarrat Rahat's north end (fig. 5) as well as at Ḥarrat I'shara-Khirsāt that lies about 115 km north-northwest of Ḥarrat Rahat (fig. 1, no. 11). In both harrats, the bases of the Tertiary volcanic sections are 300–500 m above grade, consistent with appreciable post-eruptive tectonic offsets (Calvert and Sisson, 2023). Normal faults with offsets of no more than a few meters cut a 2.1-Ma lava flow exposed 1 to 2 km to the northeast of Ḥarrat Rahat's northeast end. The faulted lava flow probably vented from the southern periphery of Ḥarrat Khaybar but possibly from Ḥarrat Kuramā' (Downs and others, 2019; Robinson and Downs, 2023). Observations are too few to assign rates of offset and their changes, but extensional tectonism that diminished from the Miocene to the present accords with the observation that early, large volume Ḥarrat Rahat lava flows drape the Great Escarpment with little or no faulted offsets (Camp and Roobol, 1989, 1991a; Ball and others, 2023; Calvert and Sisson, 2023). Roobol and Camp (1991a) and Camp and others (1991) interpret from geological and geomorphic evidence that Ḥarrat Khaybar's main vent axis also overlies a north-south striking, down-to-the-west fault.

Ḥarrat ash Shamā, in northwestern Saudi Arabia, Jordan, and Syria, also shows clear correspondence between vent orientations and tectonic structures (Ilani and others, 2001). The harrat has high-standing vent loci that are elongate north-northwest to south-southeast, some of which are aligned in series, and others similarly oriented, that are offset laterally to the west (fig. 4). The harrat is flanked on its southwest side by the al Azraq-Wādī as Sirhān graben complex and on its east by the Umm Wu'al graben, both of which are defined by bounding faults that also strike north-northwest to south-southeast. These relations are consistent with the high-standing vent loci having developed above similarly striking extensional faults. Smaller, more westerly striking grabens and surface fractures are also present, and subordinate west-northwest to east-southeast trending vent alignments match those orientations (Bender, 1975), showing that magmas exploited shallow basement weaknesses of various orientations.

[2]Rock chemical compositions recast into weight percent of rock-forming minerals by the method of Cross, Iddings, Pirsson, and Washington (CIPW).

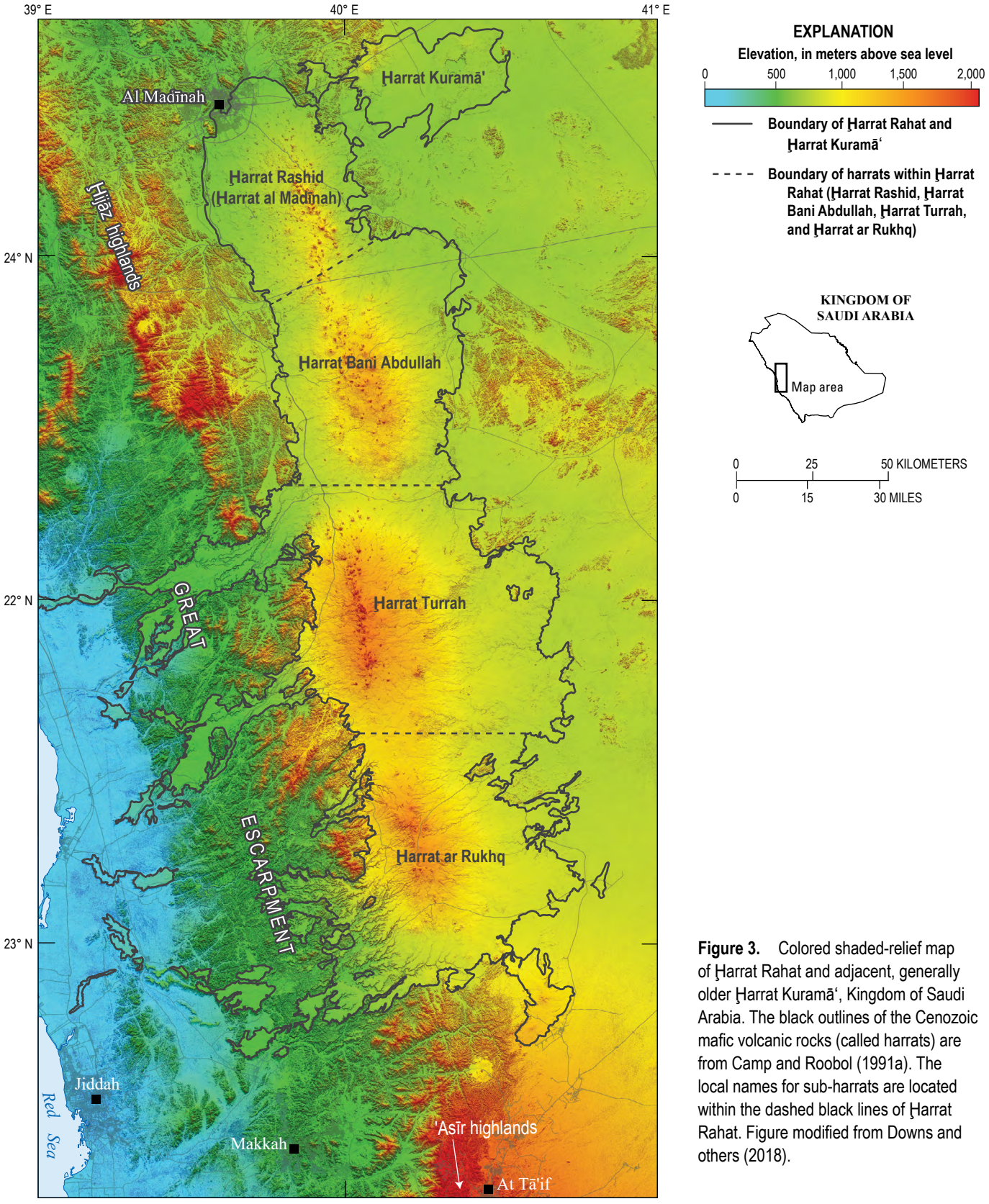

Shaded-relief and shoreline from 12-meter TanDEM-X digital elevation model acquired from German Aerospace Center, 2017

Figure 3. Colored shaded-relief map of Ḫarrat Rahat and adjacent, generally older Ḫarrat Kuramā‘, Kingdom of Saudi Arabia. The black outlines of the Cenozoic mafic volcanic rocks (called harrats) are from Camp and Roobol (1991a). The local names for sub-harrats are located within the dashed black lines of Ḫarrat Rahat. Figure modified from Downs and others (2018).

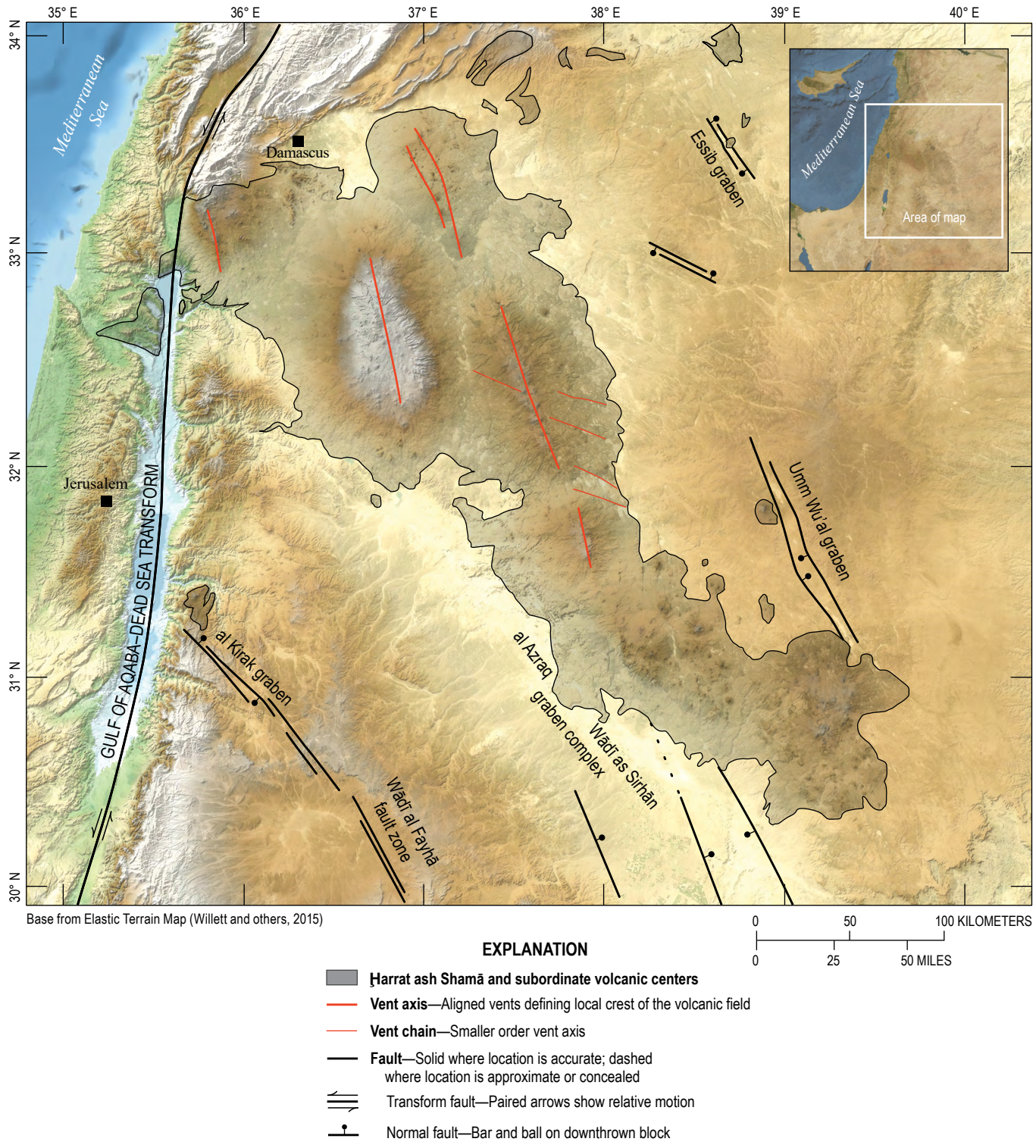

Figure 4. Colored shaded-relief map of Ḫarrat ash Shamā, Syria, Jordan, and vicinity. Geology from Bender (1975), Coleman and others (1983), Ponikarov and Mikhailov (1986), Meissner and others (1990), and Sneh and others (1998).

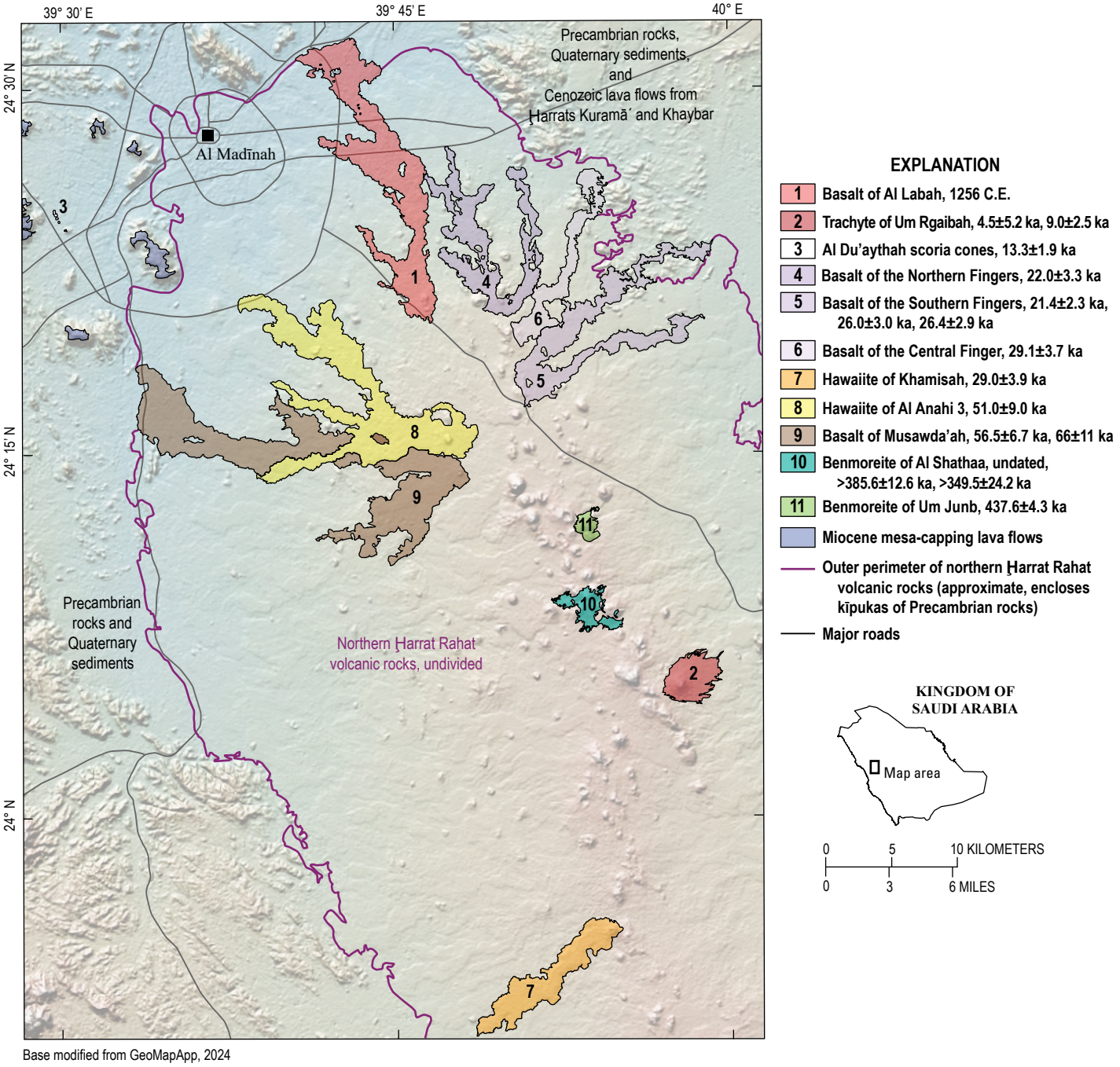

Figure 5. Colored shaded-relief map of northern Ḫarrat Rahat near Al Madīnah, Kingdom of Saudi Arabia, showing the 1256 Common Era (C.E.) basalt of Al Labah lava flow and some older volcanic deposits. Basalts of the Northern, Central, and Southern Fingers, the hawaiite of Khamisah, and a portion of the hawaiite of Al Anahi 3 were previously interpreted as post-Neolithic (Camp and Roobol, 1989, 1991a) but with direct dating proved to be late Pleistocene. Geology modified from Downs and others (2019) and Robinson and Downs (2023). Eruption age determinations (in thousands of years ago [ka] with one standard deviation uncertainties) are from Stelten and others (2023). Base topographic image generated with GeoMapApp (https://www.geomapapp.org) using the global multi-resolution topography of Ryan and others (2009).

Notably, the vent axes of harrats on the Arabian Shield are not oriented perpendicular to the Arabia Plate's direction of motion as determined from geodetic measurements (Reilinger and others, 2015), so although the Arabia Plate may be extending in its direction of motion, as for slab pull as it subducts beneath Eurasia, other factors are influencing fault directions and vent alignments, potentially including the flexure of the uplifted shield's western portion (Calvert and Sisson, 2023).

Volcanic Landforms and Eruptive Styles

Basalts

Harrat eruptions are dominantly effusions of alkali basaltic lavas that form flows with lengths in the range of 2.5–55 km (for example, the Habir flow of Ḥarrat Khaybar) with individual flow-field widths commonly of 0.25–5 km. Minimal incision prevents directly measuring thicknesses of many young-appearing flows, but simple assumptions about preexisting topography give approximate average thicknesses in the range of 2–8 m for flows of common areal extents, leading to volumes estimated for individual flows in the tenths of cubic kilometers (Dietterich and others, 2018, 2023).

Further analysis derives eruption durations of 1–15 weeks (Dietterich and others, 2018, 2023), similar to the 52 days observed for northern Ḥarrat Rahat's 1256 Common Era (C.E.) eruption near Al Madīnah (Camp and others, 1987). Young-appearing basaltic lava flows can have well defined channels, levees, and pāhoehoe surfaces close to their vents but with distance commonly transform to ʻaʻā. Some early Pleistocene and older basaltic eruptions were considerably larger, producing flows with lengths reaching about 100 km with wadi incisions now exposing thicknesses of 50–100 m (Camp and Roobol, 1989, 1991a; Ball and others, 2023; Calvert and Sisson, 2023). Mafic scoria cones can be as small as about 150 m across at their base by 30 m high to rarely larger than 1 km across by 100 m high. Notable is that aprons of mafic tephra are absent except around definitively young vents such as that for the 1256 C.E. northern Ḥarrat Rahat eruption (Kawabata and others, 2015) and for the (possibly) 641 C.E. eruptions of Jabāl Qidr and Jabāl Habir of Ḥarrat Khaybar (Camp and others, 1991; Roobol and Camp, 1991a). The region can be windy, and infrequent rainstorms can be quite heavy, so thin, fine tephras probably simply blow or wash away.

Hawaiites and Mugearites

Hawaiites range from indiscernibly different from the alkali basalts in their volcanic landforms to distinctly broader and flatter flows with steep flow fronts 5–15 m high and with prominent ogives on their flow surfaces. Mugearites consistently share these distinctions, consisting of steep-fronted, broad lava flows decorated with hornitos and (or) ogives. Frontal lobes of mugearite lava flows are commonly fan shaped and 1–3 km across, and although mapped mugearite flows reach 16 km in length (Downs and others, 2019; Robinson and Downs, 2023), most are no longer than 10 km. Mugearites never form the narrow, sinuous lava streams of the basalts and some hawaiites that thread down wadis and through narrow gaps between hills of Precambrian basement. Vents for mugearites, and consequently their flows, are mainly restricted to the higher elevation, volcanically more productive portions of harrats where even more evolved magmas also erupt.

Benmoreites

Benmoreites form lava flows, lava domes that transition to flows, and rarely, tuff sheets produced from pyroclastic flows. Benmoreite lava flows of northern Ḥarrat Rahat reach 7 km long with individual flow lobes 0.25–3 km across, but none are sufficiently young to preserve their original surface features. Benmoreite lava domes are 1–2 km across, stand 100–250 m above their surroundings, and can merge into short, thick flows, such as the Um Junb dome flow of northern Ḥarrat Rahat (fig. 5; Downs and others, 2019; Robinson and Downs, 2023). Portions of the outer flanks of benmoreite domes are mantled with poorly bedded tuff breccia formed of juvenile blocks and finer debris cascaded from growing domes. One dominantly benmoreitic tuff sheet is present in the northern Ḥarrat Rahat study area, this having erupted as a pyroclastic flow from the Al Shathaa volcanic center (fig. 5; Downs and others, 2019; Robinson and Downs, 2023). The tuff sheet is not large, blanketing an area only approximately 3 km by 5 km across and, where incised to its base, is revealed to be only about 5 m thick. Brenna and others (2019) discuss the petrogenesis of the trachyte-benmoreite tuff of Al Shathaa, focusing on the discovery and interesting significance of minor phonolite. Benmoreitic tephra-fall deposits are nearly absent, one pumiceous fall having been found near the foot of the Um Junb dome flow about 1 km from the vent and consisting of a layer only about 0.5 m thick of finely vesicular, nearly aphyric benmoreite lapilli. Northern Ḥarrat Rahat's benmoreite vents are restricted exclusively to the area of greatest constructional volcanic relief.

Trachytes

Trachytes consist of lava domes, tuff cones, and of tuff sheets deposited from small-volume pyroclastic flows; effused trachytes were insufficiently mobile to form lava flows. Trachyte lava domes are about 0.75–2 km across and stand as high as 300 m above their immediate surroundings. Some are partly mantled with trachytic tuff breccias that were cantilevered up to steep outward dips by continued inflationary growth of the associated underlying dome; fragments of older lava flows have similarly been captured and uplifted. Four protrusions in northern Ḥarrat Rahat are interpreted as cryptodomes formed by shallow intrusions of trachytic magma that uplifted the terrain without breaching the surface. Collapse of active dome flanks formed some trachytic tuff sheets, but trachytic tuff sheets also surround open craters and low tuff cones that lack lava domes. In these localities, pyroclastic flows and their resulting tuff sheets clearly formed by direct explosive venting rather than by dome collapse. Sizes of such open craters range from as small as 0.25 km across and 20 m deep to as large as 1.7 km across and as deep as 100 m. Nested craters are common, indicating complex eruptions. The trachytic tuff

sheets are also relatively small, commonly reaching only 2–5 km from their source vents as preserved continuous deposits, although distal erosional remnants indicate primary extents may have been twice as great. Wadi incisions show that individual tuff sheets are about 2–5 m thick, with as many as several conformable or disconformable tuffs exposed in wadi walls. Trachyte pumice-fall deposits are present but are few and thin (<1 m) even within only several kilometers of source vents. Collectively, these observations point to small-volume, shallowly explosive eruptions with low plumes, not sustained Plinian or sub-Plinian plumes that would produce pumiceous fall deposits of substantial thickness and extent. Like benmoreites, trachyte vents are restricted to regions with the greatest constructional volcanic relief, or to the flanks of those regions.

Comendites (Peralkaline Rhyolites)

More evolved still are the comendites (peralkaline rhyolites) of the higher elevations of Ḩarrat Khaybar (Camp and others, 1991; Roobol and Camp, 1991a). Conspicuous among these are the comendite tuff cone of Jabāl Bayda and the comendite lava dome of Jabāl Abyad that stand out so white against the surrounding black harrat basalts that they were conjectured to be scoria cones blanketed with snow (Richard and Neumann van Padang, 1957). The tuff cone of Jabāl Bayda is 1.5 km across, crater rim to crater rim, and about 3 km across at its base, standing as high as 180 m above its flanking rocks, with its crater floor 40–80 m below the crater rim. A small comendite lava dome consisting of two lobes, each about 250 m across and 5–20 m high, is centered in the crater floor. The exposed portion of the comendite dome of Jabāl Abyad is about 750 m across and stands about 300 m above surrounding rocks, but the dome's outer surface is mantled widely by coherent comendite tuff breccia formed from blocks and finer debris shed from the growing dome, and the aggregate deposit is about 2.5 km across at its base. Neither these nor other comendites of upper Ḩarrat Khaybar are surrounded by tuff sheets, indicating eruptions of insufficient volume and explosivity to produce more than minor pyroclastic flows.

Other Differentiates

Other extreme differentiates are exceptionally rare phonolite lava domes and lava flows of Ḩarrat Kurá (Camp and others, 1991; Roobol and Camp, 1991a) and Ḩarrat al Kishb (Roobol and Camp, 1991b; Camp and others, 1992). The phonolite lava dome of Ḩarrat Kurá is old, eroded, and isolated by younger basalts, so little can be said about its original landform other than that it is about 2.5 km across and stands 200 m above its surroundings. The youngest phonolite lava flows of Ḩarrat al Kishb are distinctive within the region as thick, blocky-surfaced, small flows reaching 2–3 km long, 1.5–2 km across in their lower portions, with broad ogives on their flow surfaces, and with steep, rubbly flow fronts that stand 20–70 m above adjacent older rocks. Tuff sheets are absent associated with the phonolite lavas and, unlike many trachytes and comendites, open craters are lacking at their vents. Small-volume effusions of viscous lava with little explosive component appear to typify dominantly phonolite eruptions.

Young Volcanism—Historical and Potentially Historical Events

Distinctly young-appearing lava flows, scoria cones, and small edifices are scattered across the Arabian Peninsula and stand out in the field and on aerial imagery by their stratigraphically uppermost positions within harrats, distinctly near-black colors, and pristine constructional volcanic landforms and the absence or small sizes of dust ponds and other sediments accumulated on their surfaces. Older flows characteristically erode to smooth, reddish-brown pediments of interlocking jointed lava blocks and are incised by wadis that cut through and expose multiple flows. The early development of cities and writing across the greater Middle East provides hints of observed eruptions recorded earlier than in many parts of the world, but the accounts focus on other topics and most lack sufficient detail to identify a particular location or age. For example, Moritz (1923) and Neumann van Padang (1963) comment that the biblical events asserted in Exodus 19:16 and prophesied in 18 Isaiah 34:9–10 are so like eruptions that the Israelites probably witnessed active volcanism somewhere on the Arabia Plate during their early migrations, the former event potentially being the eruption of one of the young-appearing lava flows in the juncture of Ḩarrats ar Rahá and al 'Uwayrid in northwestern Saudi Arabia (fig. 1, nos. 3 and 4). Neumann van Padang (1963) further compiles and discusses other possible historical eruptions in the region, and it is advisable to consult that work and references therein directly, as some subsequent publications and summaries have presented as certain eruptions whose ages, sites, and even validities are questionable.

The sole event with documentation sufficient to establish definitively its historical age, location, and products is the 1256 C.E. lava eruption of northern Ḩarrat Rahat adjacent to the then long-established city of Al Madīnah (fig. 5). That eruption released about 0.5 km^3 of lava emplaced over 52 days as a flow field about 23 km long (Camp and others, 1987; Kereszturi and others, 2016; Downs and others, 2018; Dietterich and others, 2018, 2023). Also in that west-central Arabian Shield area was a sparsely recorded eruption in 641 C.E., provisionally also attributed to northern Ḩarrat Rahat (Camp and Roobol, 1989, 1991a; Murcia and others, 2015) but that probably actually took place 150 km north at Ḩarrat Khaybar (Downs and others, 2018; Stelten and others 2020, 2023; Champion and others, 2023). There is also report of an eruption in that region in 640 C.E., but it is unclear if this was the same as the 641 C.E. Ḩarrat Khaybar event, but with a slight age disparity. The Ḩarrat Khaybar event was complex, and it is uncertain if it commenced the preceding year, or if there was an eruption perhaps from Ḩarrat al 'Uwayrid in 640 C.E. (fig. 1; Brown and others, 1989). Siebert and others (2010) and previous editions also list a Ḩarrat Khaybar eruption at between 600 and 700 C.E., but this is potentially the same as the 641 C.E. and possibly also the 640 C.E. event(s). Another account

summarized by Neumann van Padang (1963) mentions what was probably an eruption of Ḩarrat Lunayyir (fig. 1, no. 10) in or before 1000 C.E., but there are many fresh lava flows there, and the youngest has not been determined. Events to the south include mention in an Arabic poem of what was probably an eruption in 1253 C.E. almost certainly from Ḩarrah es-Sawād (or Ḩarrah Shuqrā) 130 km to the east of Aden (fig. 1, no. 24; Moritz, 1923; Wissmann and others, 1943; Neumann van Padang, 1963). Two early historical eruptions in Yemen took place from Ḩarrat Arhab about 30 km north of Ṣan‘ā‘ (fig. 1, no. 20). One is bracketed approximately at 400–600 C.E., and the other only as more recent than 200 C.E. Moritz (1923) reports a witnessed eruption near “Killis” in northern Syria in 1222 C.E. (the modern communities are the nearby Ḩawār Killis, northern Syria, and Kilis, southern Turkey), referencing this to the Arabic document Jākūt Mu‘g IV (presumably v. IV of Kitāb Mu‘jam al-Buldān [Dictionary of Countries] by Yāqūt al-Ḩamawī, 1224–1228), but the precise location is not given.

More recently, while mapping the geography of western Yemen, H. von Wissmann was told by residents of an eruption near Dhamār (a city located about 93 km south of Ṣan‘ā‘) probably in 1937 C.E. (Wissmann and others, 1943), but details are lacking. That harrat (fig. 1, no. 22) has active solfataras (Minissale and others, 2007), and Geukens (1966) reported frequent felt seismicity, but inspection of aerial images fails to identify a non-eroded, non-sedimented lava flow or volcanic edifice of appropriately youthful appearance. Least eroded among the volcanic landforms is the rhyolitic (or comenditic) edifice of Al Lessi (also written Al Lisi and Alessi) 14.5 kilometers east of Dhamār (lat 14.545° N., long 44.535° E.). Lamare (1930) reported warm, weakly sulfurous fumaroles at Al Lessi’s summit upon which a rudimentary bath or steam house (hammam) had been constructed, as well as a stone wall that encircled the summit crater. Aerial images show the crater encircling wall remains today, ruling out any significant eruption of Al Lessi since Lamare’s pre-1937 visit. Perhaps the 1937 event near Dhamār was solely enhanced steaming or a minor release of tephra, if it indeed took place. Similarly scantly supported is a possible eruption of “Djebel Yar” at the foot of the Great Escarpment near the border between Saudi Arabia and Yemen reported by Lamare (1924, p. 6) in one sentence as having been “…été en activité il y a centaine d’années (?)” [in activity about a hundred years ago (?)] but without explanatory information. Neumann van Padang (1963) and Brown and others (1989) clarify the location as within Ḩarrat Gar‘atain near Jāzān, Saudi Arabia (fig. 1, no 19; some publications report this harrat as Tihāmat ‘Asīr, but this translates as “coastal plain of the ‘Asīr region” which hosts several harrats). No young lava flow is present in Ḩarrat Gar‘atain, and none of its volcanic cones appear in aerial images as appropriately unbreeched or uneroded as would be so for a magmatic eruption only 200 years ago. Like the possible 1937 eruption near Dhamār, this early 1800s eruption must have been quite small, if it took place at all. A widely repeated assertion of a lava lake active in 1850 C.E. at the Es Safā edifice in the southwest Syrian portion of northern Ḩarrat ash Shamā (fig. 1, no. 2) has since been discredited by the recent availability of the original reference (Wetzstein, 1860) that, while describing and sketching many volcanic landforms, nevertheless makes no mention of an event as noteworthy as encountering molten lava.

Modern events include the 2009 C.E. emplacement of a dike to near-surface depths at Ḩarrat Lunayyir (Pallister and others, 2010) that produced ground cracking and abundant felt seismicity, and the off-continent eruptions of the volcanic islands of Jabāl aṭ Ṭayr (1750±50, 1833±1, 1863, 1883, and 2007–2008, all C.E.) and Jazā’ir az Zubayr (1824, possibly 1846, 2011–2012, and 2013, also C.E.) along the southern Red Sea’s spreading axis (fig. 1, no. 28; Siebert and others, 2010). Despite the uncertainties and possible redundancies in the historical record, it is clear that the Arabian Peninsula remains volcanically active. Owing to its until recently sparse population, additional historical eruptions probably also took place but went unrecorded, or accounts of additional historical eruptions have been lost.

Young Volcanism—Prehistoric Events

Human populations were relatively high across the Arabian Peninsula and northern Africa during the early to middle Holocene owing to greater rainfall of the Neolithic pluvial interval (approximately 11–5 thousand years ago [ka]; also known as the Holocene humid period and the northern African humid period; Shanahan and others, 2015) that enabled widespread pastoral and hunting-gathering communities. Over that time, inhabitants constructed thousands of stone structures within the Arabian Peninsula and the Levant including burial mounds (large cairns), low rings (possible tent margins or other enclosures), walls adjoined in V-shapes (kites) to trap and hunt animals, and enigmatic low rectangular structures (mustatils) (Groucutt and others, 2020). Camp and Roobol (1989, 1991a), Camp and others (1991), and Roobol and Camp (1991a) recognized that such stone structures are absent atop most of the young-appearing lava flows in the harrats of west-central Saudi Arabia. Those workers also discovered a site near the ancient settlement of Khaybar, Saudi Arabia, where the young-appearing Habir lava flow overrode a Neolithic stone wall (lat 25.6331° N., long 39.4631° E.), and where that anastomosing flow had isolated numerous Neolithic stone structures in kīpukas. Another site high in Ḩarrat Khaybar was also found where young-appearing basaltic lava from Jabāl Qidr overrode Neolithic structures (lat 25.6786° N., long 39.9638° E.). From these observations, those authors (and Coleman and others, 1983) interpreted that the young-appearing lava flows lacking such anthropogenic monuments erupted after the pluvial interval, so were “post-Neolithic.” The absence of capping anthropogenic structures was then used to classify as post-Neolithic similarly young-appearing lava flows in Ḩarrats Rahat, Khaybar, Ithnayn, and al Kishb (Camp and Roobol, 1989, 1991a; Roobol and Camp, 1991a,b), and this approach has been extended to Ḩarrat Lunayyir (Al-Amri and others, 2012).

The interpretation that the many young-appearing flows had erupted within the last approximately 5,000 years was not, however, confirmed when such lava flows of northern Ḩarrat Rahat were dated directly by the ^{36}Cl exposure or $^{40}Ar/^{49}Ar$ methods. There, products of four sizeable lava eruptions previously classified as post-Neolithic but pre-historical had vented within 30 km of the center of Al Madīnah, and a fifth such lava flow erupted 67 km southeast of the city center (Camp and Roobol, 1989, 1991a). These lava flows have since been named

(Downs and others, 2019; Robinson and Downs, 2023) from south to north: the hawaiite of Khamisah, the hawaiite of Al Anahi 3, and the basalts of the Southern, Central, and Northern Fingers, the latter three being spatially, temporally, and compositionally associated as the informally named Five Fingers lava flows (for example, Dietterich and others, 2023) (fig. 5). Eruption ages measured for these are: hawaiite of Al Anahi 3, 51.0±9.0 ka (^{36}Cl); hawaiite of Khamisah, 29.0±3.9 ka (^{40}Ar/^{39}Ar); basalt of the Central Finger, 29.1±3.7 ka (^{36}Cl); basalt of the Southern Fingers, 26.4±2.9, 26.0±3.0, and 21.4±2.3 ka (^{36}Cl); and basalt of the Northern Fingers, 22.0±3.3 ka (^{36}Cl) (Downs and others, 2018, 2019; Stelten and others 2020, 2023). Additional results from that area bearing on young volcanism include: (1) an age determination on the 1256 C.E. lava flow of 810±240 years ago (^{36}Cl) that tests and supports the accuracy of the exposure-age results, (2) an age of 13.3±1.9 ka (^{36}Cl) on lava associated with a cluster of small scoria cones just to the west of Al Madīnah (fig. 5) that negates prior attribution of those cones and lava to the poorly documented 641 C.E. eruption (Camp and Roobol, 1989, 1991a), and (3) age determinations of 9.0±2.5 ka (^{36}Cl) and 4.5±5.2 ka (^{40}Ar/^{39}Ar) on the trachyte of Um Rgaibah establishing that trachyte as probably Holocene in age and refuting a previously determined age of 1.47 Ma (K-Ar; Pellaton, 1981) that was inconsistent with that trachyte's high stratigraphic position and minimal erosion. Three additional Ḥarrat Rahat lava flows from vents 92–117 km south-southeast of Al Madīnah were also classified as post-Neolithic but pre-historical (Camp and Roobol, 1989, 1991a), but these were outside the SGS-USGS focused study area so were not dated.

These results show that, other than the 1256 C.E. lava flow, all lavas in the northern Ḥarrat Rahat region previously interpreted as having erupted in the last approximately 5,000 years actually erupted well before the Neolithic pluvial interval. The absence of anthropogenic structures atop those late Pleistocene lava flows may have resulted from the fresh flows' sharp, blocky, and a'ā surfaces being inhospitable to Neolithic inhabitants who chose, instead, to live and build on the smoother eroded surfaces of nearby older lava flows. The observation that the Habir and Jabāl Qidr flows of Ḥarrat Khaybar overrode and isolated Neolithic structures establishes that some young-appearing lava flows of the region did erupt in post-Neolithic times, but the numbers of such late Holocene eruptions must be considerably fewer than previously interpreted. Since replicate measurements from the same lava flows show that the ^{36}Cl method can yield consistent and accurate results, the true ages of young volcanism across the Arabian Peninsula can now be determined directly without great difficulty.

Pleistocene Volcanism and Derived Eruption Probabilities

Northern Ḥarrat Rahat is the only volcanic center in the region studied sufficiently to reveal its detailed Pleistocene activity. Following Smith (1980, 1982), Camp and Roobol (1989, 1991a) divided the entirety of 20,000 km^2 Ḥarrat Rahat into three informal volcano-stratigraphic units, from older to younger: the Miocene to Pliocene Shawahit basalt, the Pliocene Hammah basalt, and the Quaternary Madinah basalt, with the geographic extent of volcanism becoming more restricted with decreasing age and shifting generally toward the north end of the harrat. Those authors further subdivided the Madinah basalt into seven presumed age categories based on relative degrees of erosion, sediment cover, remote-sensing spectral characteristics, and sparse K-Ar age measurements. The approximately 4,000 km^2 portion of the Madinah basalt north of latitude 24° N., corresponding to the Rashid or Al Madīnah sub-harrat (fig. 3), was remapped and dated extensively during the SGS-USGS effort that benefitted from the availability of high-resolution digital topography and aerial images, ready field access by helicopter and 4-wheel drive trucks, ^{40}Ar/^{39}Ar and ^{36}Cl geochronology, and other resources (see Sisson and others, 2023a). Key findings include that nearly all (80 percent by area) of the rocks that form the exposed surface of the study area erupted within the last 500 thousand years (k.y.), with about half of the surface rocks having emplaced in the last 300 k.y.; the oldest rocks measured in the study area erupted at 1.2 Ma (Downs and others, 2019; Stelten and others, 2020, 2023). If simple assumptions are made of the depth to the base of Ḥarrat Rahat, the exposed and dated volcanic rocks are estimated as constituting no more than approximately 20 volume percent of northern Ḥarrat Rahat's volcanic products, with the remaining approximately 80 volume percent concealed beneath younger lavas and tuffs.

Rock exposures and eruption-age determinations are sufficiently abundant for the last approximately 500 k.y. to reveal that northern Ḥarrat Rahat's volcanism was pulsed (fig. 6) with major peaks of activity in the vicinity of 450 ka and 250 ka, separated by a relative lull from about 370 to 270 ka, and that eruptions generally decreased in number since the last major peak of activity (Downs and others, 2019; Stelten and others, 2020, 2023). Activity can be subdivided more finely, albeit somewhat arbitrarily, over the last approximately 300 k.y., whereas excessive concealment prevents similarly refined subdivisions of volcanic activity for times prior to about 500 ka.

Rock exposures and age determinations for products emplaced over the last 180 k.y. are sufficiently complete to estimate eruption frequency quantitatively (Stelten and others, 2023). Using an exponential, or Poisson, probability distribution yields an average eruption recurrence of 3.2 k.y. (fig. 7), but such an approximation provides a poor fit to some lava flows that appear to have erupted in rapid succession. A mixed-exponential distribution consisting of superposed short- and long-term recurrence rates fits these events better. Average duration of the short-term recurrence interval is not defined narrowly by the measured eruption ages, but, based on similarity of paleomagnetic directions measured on lavas, clustered eruptions can be estimated as having spanned no more than a few hundred years (Champion and others, 2023). Using about 220 years as the average short-term recurrence interval, the long-term recurrence is estimated as averaging 4.0 k.y. This analysis (Stelten and others, 2023) quantifies the cautious expectation that a volcano that has just erupted may do so again soon, but after some time has passed with no eruption, the chance of an eruption decreases to some longer term value. Using the single-exponential approximation with an average recurrence of 3.2 k.y., the probability of an eruption in any 50-year period is estimated as 1.5 percent, whereas the mixed-exponential model with short- and long-term average

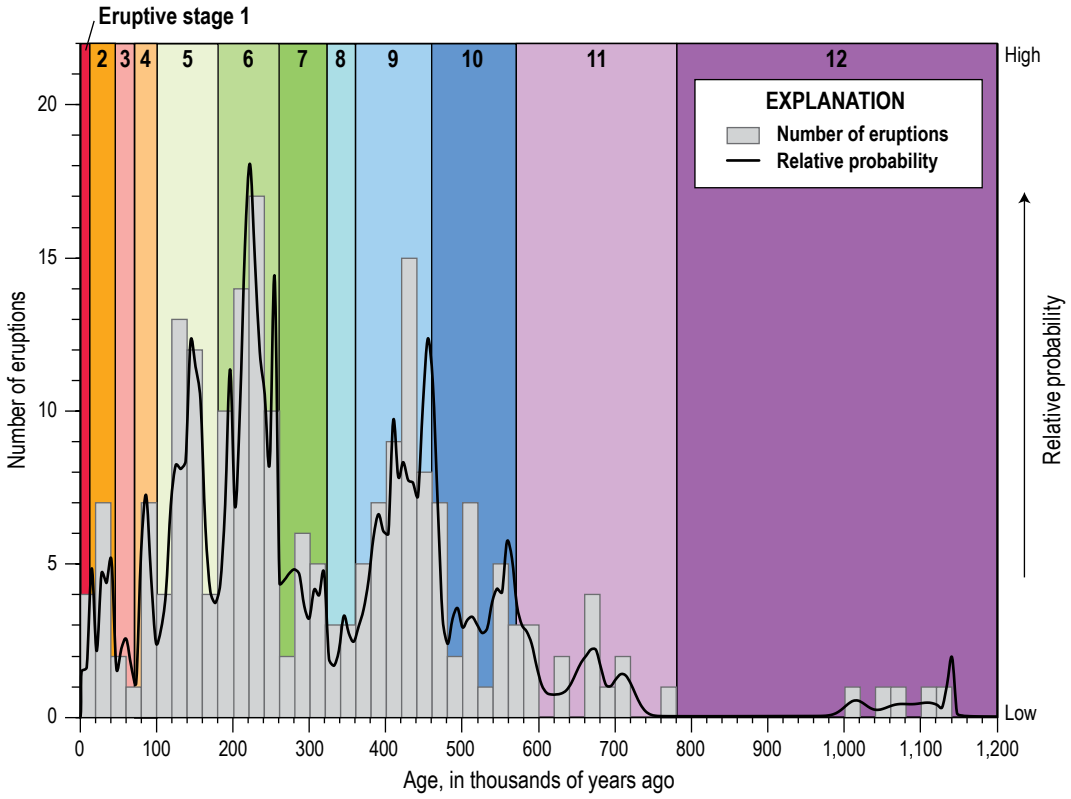

Figure 6. Histogram of eruption ages measured for volcanic rocks exposed on the surface of northern Ḫarrat Rahat, Kingdom of Saudi Arabia, and fit to a probability density function (black line) (Downs and others, 2019; Stelten and others, 2020, 2023). The volcanic geology is subdivided into 12 eruptive stages mainly centered on peaks of activity (color bands). Rock exposures and eruption-age determinations are sufficiently abundant for the last approximately 500 thousand years to reveal that northern Ḫarrat Rahat's volcanism was pulsed. However, because of concealment, resolution of eruptive activity diminishes with increasing age, producing the greater apparent durations of older stages. Figure modified from Stelten and others (2023).

recurrences of about 220 years and 4.0 k.y. gives about a 5 percent chance of an eruption in the 50-year period immediately after a prior eruption. Sufficient time has elapsed since Ḫarrat Rahat's last eruption in 1256 C.E. that the eruption probability has decreased to the long-term rate.

Runge and others (2014) inferred a minimum average eruption recurrence interval of 3.9 k.y. for the entirety of Ḫarrat Rahat by grouping exposed vents into probable eruptive events, plus estimating the numbers of events that may be concealed beneath younger products or were lost to erosion, and then assuming these eruptions spanned the harrat's approximately 10 million years of activity (Camp and Roobol, 1989, 1991a). Runge and others (2014) caution, however, that the known eruptive frequencies of basaltic volcanic fields span five orders of magnitude. This is consistent with the pulsed activity of northern Ḫarrat Rahat demonstrated by direct geochronology and geologic mapping (fig. 6), so the agreement between the Runge and others (2014) estimated minimum eruption recurrence and that determined directly for the last 180 k.y. may be largely fortuitous.

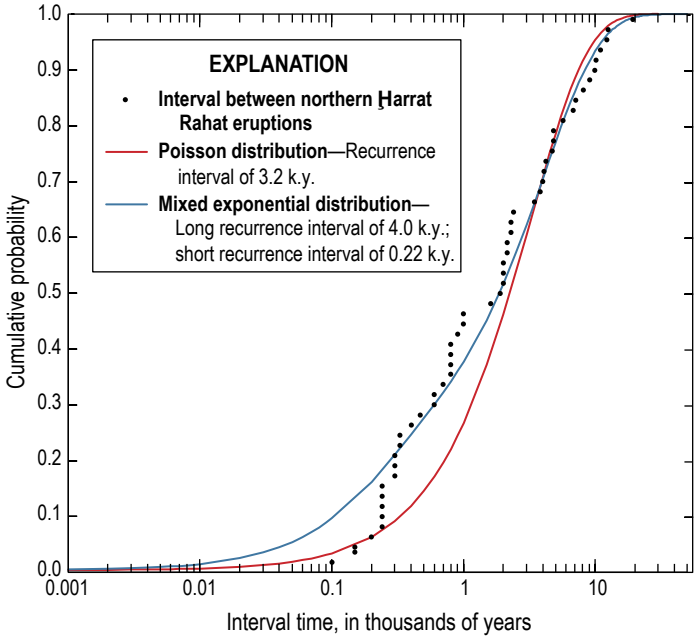

Figure 7. Plot of the durations between successive eruptions of northern Ḫarrat Rahat, Kingdom of Saudi Arabia, versus the cumulative probability of that population fit with probability functions for Poisson and mixed exponential distributions (Stelten and others, 2023). Plotted and fit results are limited to eruptions in the last 180 thousand years (k.y.) owing to a high degree of completeness in the exposed rock record and in age determinations. Figure modified from Stelten and others (2023).

Magmatic Origins—Mantle Sources and Melting Processes

Salters and others (2023) and Sisson and others (2023b) address the origins of northern Ḥarrat Rahat's basalts from the standpoints of radiogenic isotopes and trace and major elements. Northern Ḥarrat Rahat's basalts prove to be the closest among the Arabian harrats to northern hemisphere MORB with respect to their lead (Pb), neodymium (Nd), hafnium (Hf), and strontium (Sr) isotopic values but are offset from such MORB consistent with incorporation of as much as 30 weight percent of material from (or like) the Afar mantle plume. Neogene and Quaternary (post-trap) volcanic rocks of Yemen and the Gulf of Aden that erupted closer to the Afar depression show greater isotopic influences of the Afar plume, and the signature of the Dupal[3] mantle isotopic anomaly (Hart, 1984) also appears. This appearance of Indian Ocean MORB characteristics indicates that those magmas also originate mainly from sub-lithospheric sources. A dominantly depleted-mantle source for northern Ḥarrat Rahat, similar to that of ordinary MORB, is also indicated by inversion of the basalts' trace element concentrations (fig. 8), following the method of Minster and Allègre (1978), but that the extent of melting is considerably less than for MORB, averaging only a few percent (Sisson and others, 2023b); this low degree of melting accounts for the harrat basalts' alkalic character. Concentration ratios of certain trace elements define fields that are intermediate between trends expected for partial melting of garnet and spinel peridotite (fig. 9) (Salters and others, 2023). Major-element compositions of northern Ḥarrat Rahat's most magnesian basalts are also similar to those of liquids expected for melting deep in the spinel peridotite stability field, if those basalts' compositions are adjusted for modest (~8 weight percent) olivine fractionation (Sisson and others, 2023b). Consistent with this are mantle potential temperatures derived as being 1,345–1,390 degrees Celsius (°C), similar to values estimated for the source of common MORB (Sarafian and others, 2017).

Collectively, these results support a relatively simple scenario wherein chemically depleted asthenospheric upper mantle peridotite, mixed with subordinate materials from (or like) the Afar mantle plume, upwells beneath the axis of the harrat belt and melts to small extents as it passes from the garnet to spinel stability fields. Melting does not continue to shallow depths in the spinel field, unlike MORB, so most

[3]A region of the Indian and south Atlantic Oceans where midocean ridge basalts have elevated $^{208}Pb/^{204}Pb$ and $^{207}Pb/^{204}Pb$ values relative to midocean ridge basalts of the northern hemisphere and Pacific Ocean.

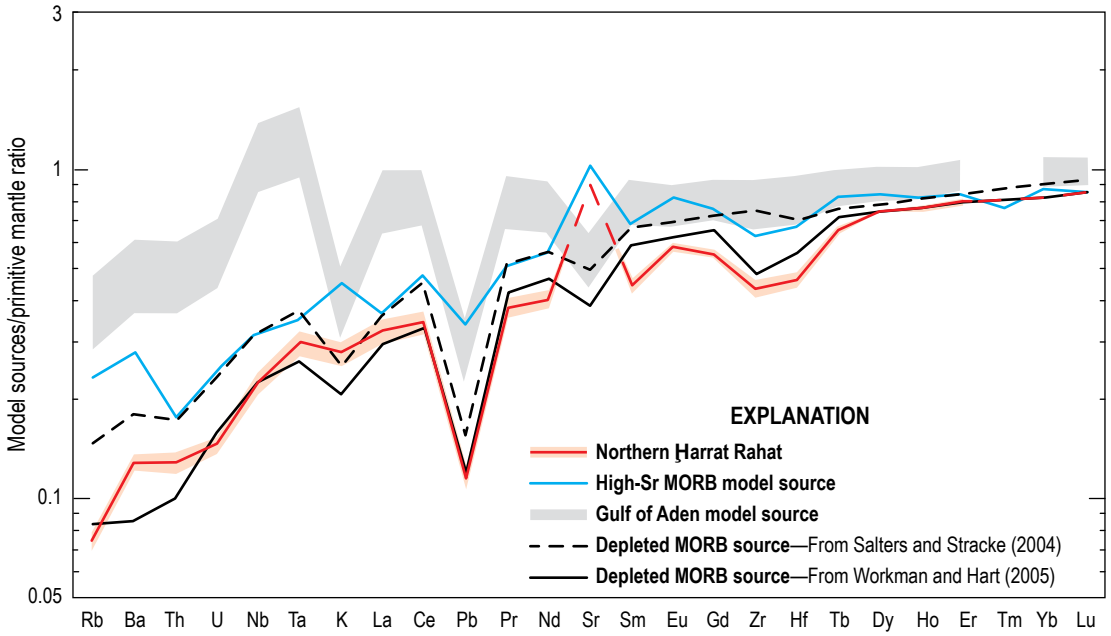

Figure 8. Plot of the trace element composition of the mantle source of northern Ḥarrat Rahat basalts, Kingdom of Saudi Arabia, inferred by the method of Minster and Allègre (1978). This is compared with estimates for the source of common, chemically depleted midocean ridge basalts (MORB), distinctly strontium (Sr)-rich MORB, and an estimate for the source of Gulf of Aden basalts that erupt close to the inferred center of the Afar mantle plume. Compositions are plotted with concentrations normalized to (divided by) the primitive mantle composition of Sun and McDonough (1989). Source concentration for Sr (dashed part of red line) for northern Ḥarrat Rahat was derived using a modified method described by Sisson and others (2023b). Figure modified from Sisson and others (2023b).

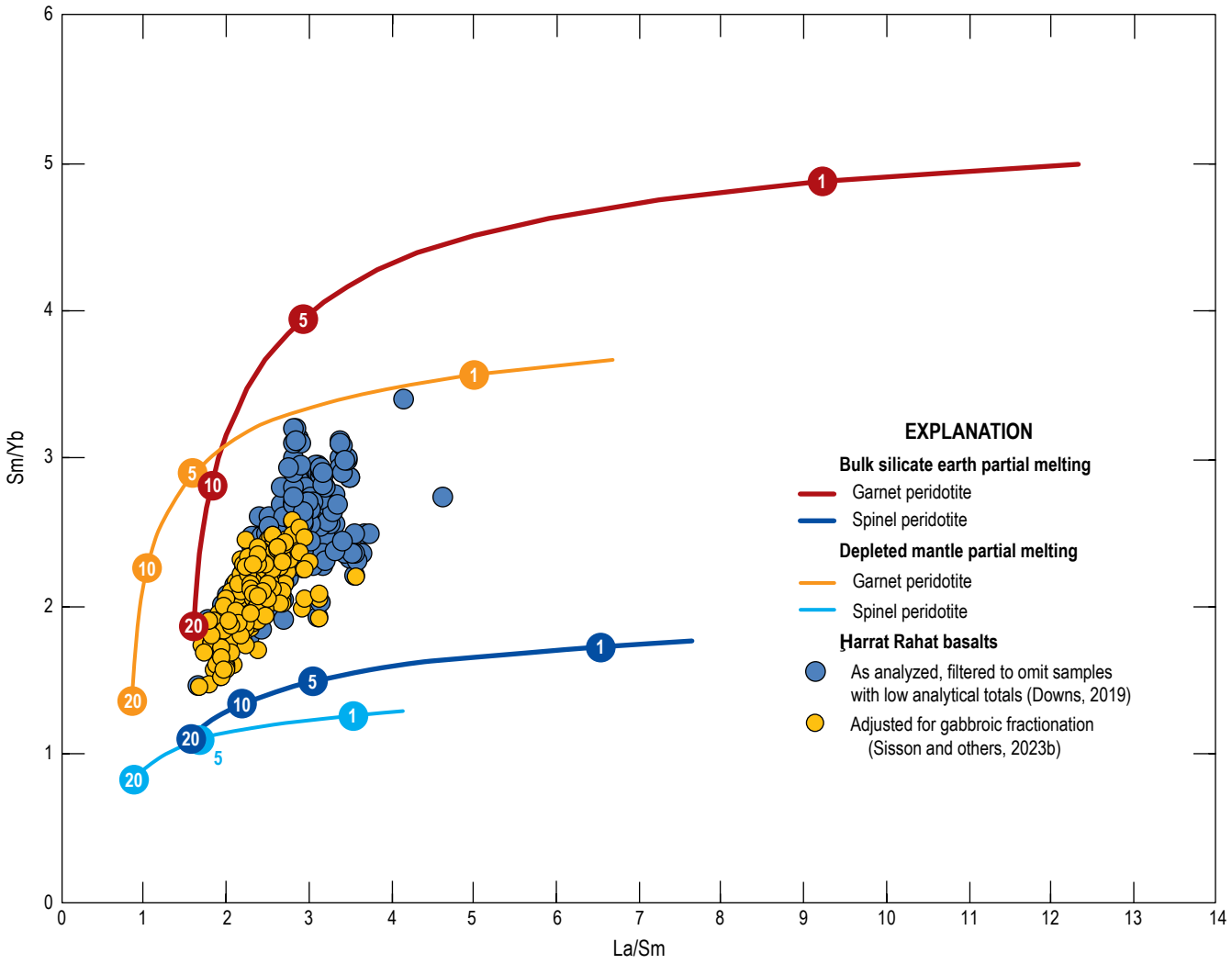

Figure 9. Plot of La/Sm versus Sm/Yb, in weight concentrations, for spinel- and garnet-facies peridotite partial melting compared with Ḫarrat Rahat basalts, Kingdom of Saudi Arabia. Harrat samples are filtered to include only those with MgO greater than or equal to (≥) 6.8 weight percent and P_2O_5/K_2O less than (<) 0.8 and are adjusted to primitive compositions by reversing gabbroic fractionation. Curves show partial melting behavior of depleted mantle and bulk silicate earth compositions in the garnet and spinel peridotite stability fields. Melting curves span from 0.1 to 20 weight percent and numbered circles mark melt fractions of 1, 5, 10, and 20 weight percent. See Salters and others (2023) for mineral/melt partition coefficients, source modes, and melting reactions. Figure modified from Salters and others (2023).

liquids remain alkalic. That melting ceases deep in the spinel field is consistent with upwelling having impinged on the base of the Arabia Plate lithosphere. Segregation pressures deep in the spinel field of 1.8–2.0 gigapascals (GPa) (Sisson and others 2023b) would place this at depths of approximately 60–70 km, consistent with detection of the lithosphere-asthenosphere boundary in that depth range beneath the main harrat belt both by magnetotellurics (Bedrosian and others, 2019; Peacock and others, 2023) and by seismic receiver functions (Blanchette and others, 2018). This is, however, considerably shallower than the depth expected for the base of Neoproterozoic lithosphere (Artemieva, 2006), a topic that will be addressed subsequently.

Magmatic Origins—Crustal Differentiation

The origin of northern Ḫarrat Rahat's basalt-hawaiite-mugearite-benmoreite-trachyte compositional spectrum is relatively simple. The magmas erupt through the Neoproterozoic Arabian Shield, so crustal assimilation is to be expected. This is confirmed by Pb isotopes that shift toward the common-Pb values of exposed shield rocks as magnesium oxide (MgO) concentrations or Mg numbers (Mg# = molar Mg/[Mg+Fe^{2+}]) of the volcanic rocks decrease (Salters and others, 2023). The shifts are, however, small (fig. 10) and can be accounted for by no more than 5 weight percent assimilation upon attaining trachytic magma compositions. Low extents of assimilation are also indicated by trace element ratios that fail to shift toward continental crustal values with progressive differentiation (fig. 11). Instead, crystallization differentiation, broadly defined, is the dominant differentiation process, accompanied by mixing between more and less evolved magmas and by interactions between earlier and later magmatic intrusions (Sisson and others, 2023b).

Differentiation of basalts through hawaiites has been investigated thoroughly because those magmas dominate erupted volumes (Sisson and others, 2023b). Magnesian alkali basalts (to nearly 13 weight percent MgO) differentiate by olivine fractionation to approximately 10 weight percent MgO whereupon

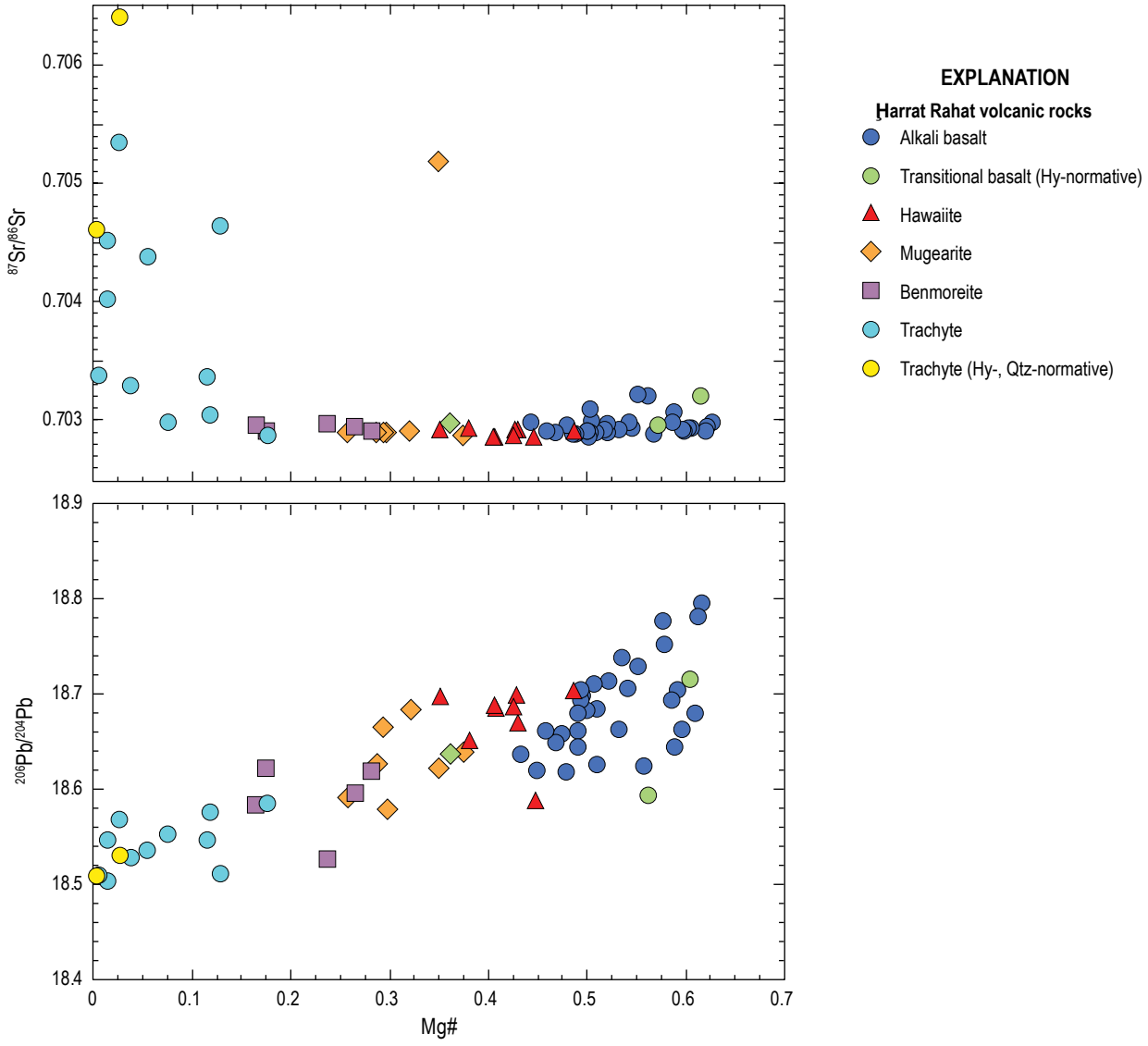

Figure 10. Plots of magnesium (Mg) number (Mg#=Mg/[Mg+Fe^{2+}], molar) as a fractionation index versus Sr and Pb isotopic compositions for Ḫarrat Rahat volcanic rocks, Kingdom of Saudi Arabia. The continuous decrease in $^{206}Pb/^{204}Pb$ with the fractionation index (decreasing Mg#) indicates that crystallization differentiation of Ḫarrat Rahat magmas was accompanied by progressive crustal contamination. The relatively constant $^{87}Sr/^{86}Sr$ compositions except at low Mg# indicates that the crustal contaminant had little influence on the magmatic $^{87}Sr/^{86}Sr$ until alkali feldspar fractionation reduced the Sr concentrations of the magmas. Other abbreviations: Hy, hypersthene; Ne, nepheline; Qtz, quartz; all in the CIPW norm defined as rock chemical compositions (recast into weight percent) of rock-forming minerals, following the method of Cross, Iddings, Pirsson, and Washington (CIPW). Figure modified from Salters and others (2023).

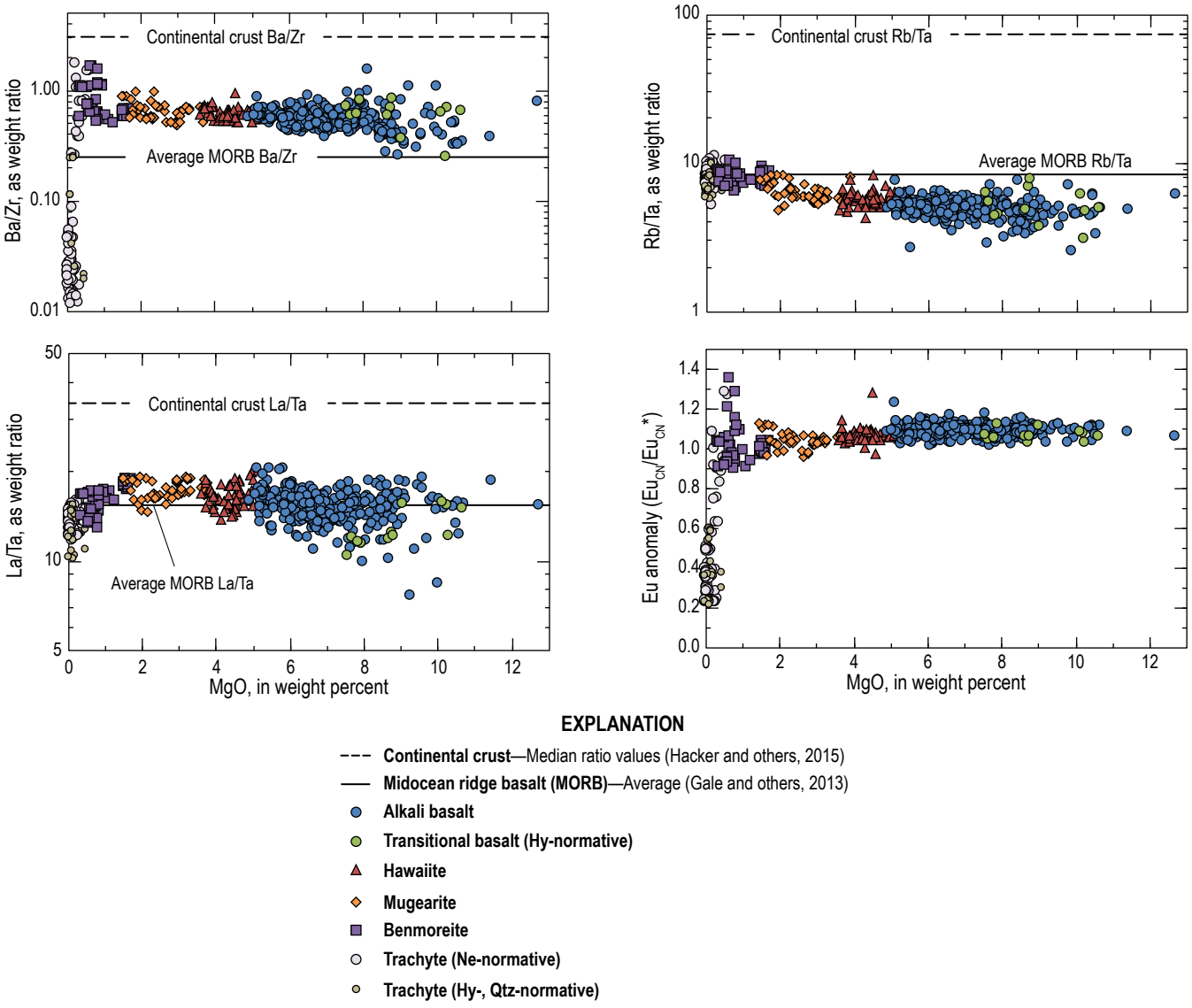

Figure 11. Plots of trace-element weight concentration ratios versus MgO concentration for Ḥarrat Rahat volcanic rocks, Kingdom of Saudi Arabia (Downs, 2019; Sisson and others, 2023b), compared with values for continental crust and average midocean ridge basalt (MORB). Also plotted is the europium (Eu) anomaly, defined as Eu_{cn}/Eu^{*}_{cn} where subscript cn indicates concentration normalized to (divided by) its concentration in chondritic meteorites (O'Neill, 2016), and Eu^{*}_{cn} is defined as $\sqrt{Sm_{cn} \times Gd_{cn}}$. This measures the deviation of a sample's Eu concentration from a value expected for a smooth chondrite-normalized rare earth element pattern. Other abbreviations: Hy, hypersthene; Qtz, quartz in the CIPW norm, defined as rock chemical compositions (recast into weight percent) of rock-forming minerals, following the method of Cross, Iddings, Pirsson, and Washington (CIPW); all other rocks are nepheline (Ne) normative. Figure modified from Sisson and others (2023b).

olivine gabbroic fractionation commences; this continues to approximately 6–7 weight percent MgO, at which point titanomagnetite joins the crystallizing assemblage. Concentrations of SiO_2 of bulk magmas (approximately that of the melt) decrease modestly during the initial olivine gabbroic crystallization interval, but SiO_2 concentrations then increase once titanomagnetite joins the crystallizing assemblage. Crystallization of the olivine+titanomagnetite gabbroic assemblage continues through the hawaiites. Most of the basalts are mixtures, however, obscuring simple liquid lines of descent (fig. 12). Using enrichments of the highly incompatible elements thorium (Th), tantalum (Ta), uranium (U), and niobium (Nb) as indices of differentiation, and referencing to the median alkali basalt of northern Ḥarrat Rahat with Mg#>0.64 as the parent (Downs, 2019; Sisson and others, 2023b), titanomagnetite appears after about 60 weight percent crystallization, and the median hawaiite would result from about 75 weight percent crystallization. Apatite joins the crystallizing assemblage within the mugearites, shown by its appearance as microphenocrysts, and alkali feldspar joins and comes to dominate the crystallizing assemblage near the benmoreite-trachyte transition. Using the same parent and enrichments of highly incompatible elements, the extent of solidification to

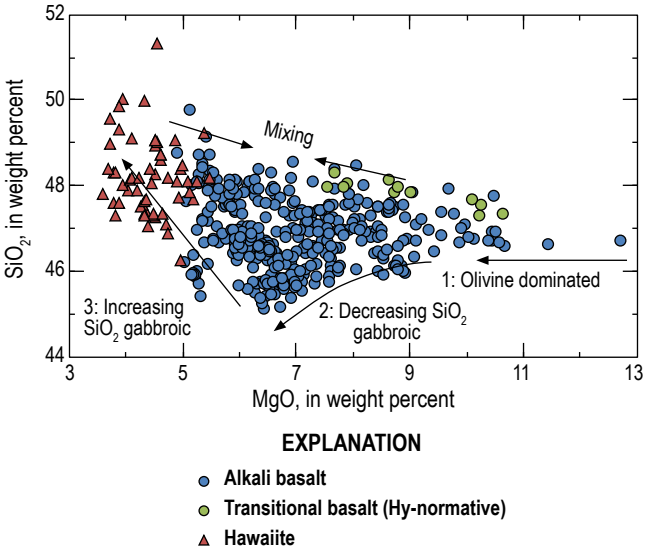

Figure 12. Plot of MgO versus SiO_2 concentrations, in weight percent, for basalts and hawaiites of northern Ḫarrat Rahat (Downs, 2019; Sisson and others, 2023b), Kingdom of Saudi Arabia, showing three stages of crystallization-differentiation: (1) olivine dominated, (2) olivine gabbroic, and (3) titanomagnetite (Ti-magnetite) olivine gabbroic. This illustrates that most basalts are mixtures between the bounding fractionation trajectories. Other abbreviations: Hy, hypersthene in the CIPW norm, defined as rock chemical compositions (recast into weight percent) of rock-forming minerals, following the method of Cross, Iddings, Pirsson, and Washington (CIPW); all others are nepheline normative. Figure modified from Sisson and others (2023b).

form the median mugearite is estimated as 83 weight percent, the median benmoreite as 86 weight percent, and the median trachyte as 95 weight percent. Some mugearites, hawaiites, and low-MgO basalts of northern Ḫarrat Rahat have P_2O_5/K_2O values appreciably greater than those of high-MgO basalts, inconsistent with simple, progressive crystallization-differentiation, but the anomalously high P_2O_5/K_2O values can result from those magmas having assimilated apatite-bearing cumulates produced from more evolved members of the harrat magmatic system (Sisson and others, 2023b). Re-assimilation of apatite-free cumulates is probably also common but cannot be recognized as readily.

Differentiation depths are not closely defined, but results of thermodynamic modeling are consistent with magmas mainly lodging and differentiating in the mid-crust or modestly deeper (Sisson and others, 2023b), and certainly not in the upper crust, in accordance with the absence of fumaroles or other surface geothermal features and a historical lack of upper crustal seismicity. Repetitive eruptive sequences of basalt through mugearite or benmoreite to trachyte of the Matan volcanic center of northern Ḫarrat Rahat point to events of progressive differentiation and provide estimates for their durations (Stelten and others, 2018). However, rocks of the nearby Al Efairia volcanic center do not show similar temporal-compositional sequences (Downs and others, 2023) indicating more complex differentiation processes. Consistent across all the major harrats, however, is that intermediate and evolved magmas have mainly erupted from the areas with the greatest aggregate constructional volcanic relief. The high relief of such areas is evidence that those are the sites of the greatest long-term magmatic fluxes. Such areas are expected to be underlain by the most numerous and voluminous associated crustal intrusions that yield intermediate and evolved melts both by direct, progressive crystallization-differentiation and by partial remelting upon magmatic replenishment (Stelten and others, 2020, 2023). Magnetotelluric and seismic imaging have failed to detect magma reservoirs at any depth in the crust beneath Ḫarrat Rahat (Bedrosian and others, 2019; Civilini and others, 2019; Peacock and others, 2023), indicating that such intrusions are too poor in melt, too small, or both, to be resolved by the applied methods.

Geophysical Imaging and a Tectono-Magmatic Synthesis

The Arabia Plate consists mainly of Neoproterozoic rocks that assembled and stabilized by 750 Ma in its eastern portion (now largely concealed by the Arabian Platform) to 550 Ma in western parts where they are exposed in the Arabian Shield (Stern and Johnson, 2010). Applying the simple and area-weighted regressions between lithospheric thickness and terrane age of Artemieva (2006) yields expected lithospheric thicknesses in the east of at least 124 km (simple regression) or 132 km (weighted), and in the west of either at least 116 km or at least 126 km. Consistent with these is an estimate of 150 km to the base of the lithosphere in the southeastern portion of the Arabia Plate based on heat flow measurements in Oman, Saudi Arabia, and central Yemen (Rolandone and others, 2013). Using synthetic receiver functions, Hansen and others (2007) obtained similar depths to the lithosphere-asthenosphere boundary of 134–162 km beneath the Arabian Platform (median 144 km), but 69–123 km beneath the Arabian Shield including the major harrats (median 101 km), 52–78 km beneath the coastal plain and Great Escarpment (median 62 km), and 54–67 km beneath the Gulf of Aqaba-Dead Sea Transform fault system (median 63 km). Inversion of teleseismic wave travel times shows a belt of anomalously slow seismic velocity in the asthenospheric upper mantle centered beneath the most active harrats (Chang and others, 2011; Hansen and others, 2012; Yao and others, 2017), broadly underlying the pronounced shallowing of the lithosphere-asthenosphere boundary beneath the Arabian Shield (figs. 13 and 14). Magnetotelluric measurements independently detect the lithosphere-asthenosphere boundary as only at 70 km depth beneath northern Ḫarrat Rahat (Bedrosian and others 2019; Peacock and others, 2023). Thus, the mantle lithosphere beneath the belt of the most active harrats is thinner by approximately 50–80 km than would be expected for its age, defining an arch along the lithosphere's basal contact with the underlying asthenosphere. Notably, this arch and its overlying belt of voluminous harrats do not match the locations and orientations of terrane boundaries or other structures exposed on the Arabian Shield (Stern and Johnson, 2010; Johnson and Kattan, 2012).

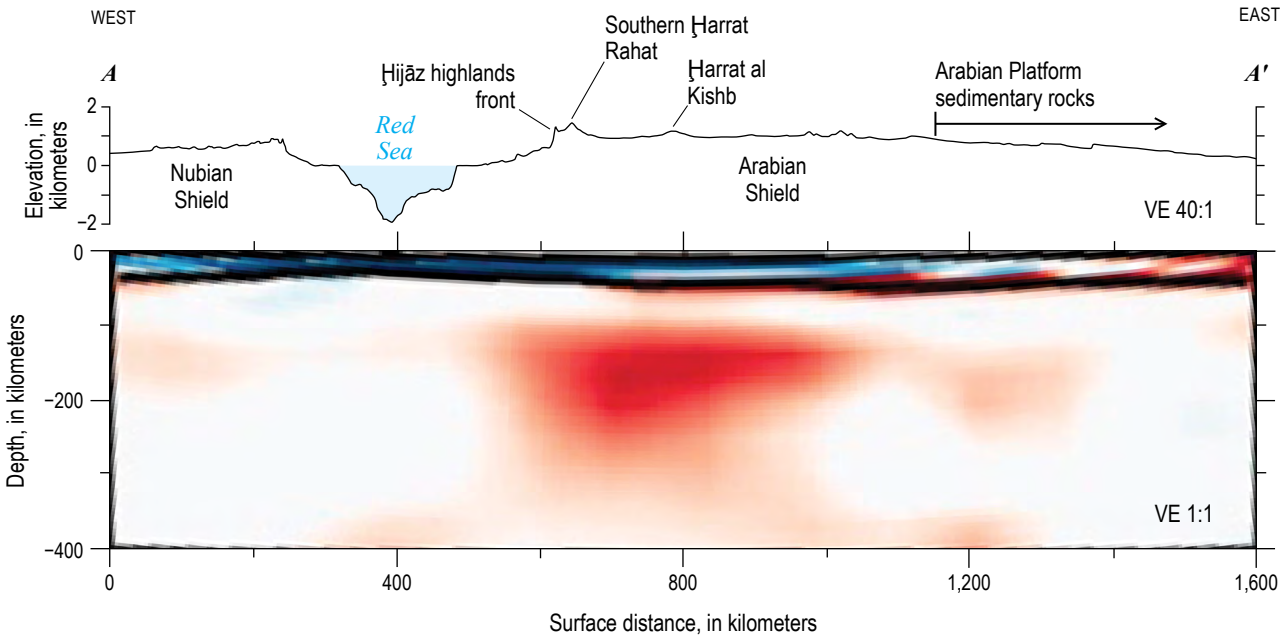

Figure 13. Topographic and geophysical cross section *A*–*A*' (refer to fig. 1 for location) is perpendicular to the Red Sea near latitude 23° N., across parts of the Nubian and Arabian Shields. Shown in varying hues are perturbations of shear-wave upper-mantle velocity relative to a reference velocity. Red, 300 meters per second (m/s) decrease, anomalously slow; blue, 300 m/s increase, anomalously fast (modified from Chang and others, 2011). Topographic profile with 40:1 vertical exaggeration (VE) created using GeoMapApp (https://www.geomapapp.org) and global multi-resolution topography and bathymetry of Ryan and others (2009). Figure modified from Calvert and Sisson (2023).

Restoring the Arabia Plate and the Sinai and Somali blocks to their positions relative to the Africa Plate prior to openings of the Red Sea and Gulfs of Aden, Aqaba, and Sinai places the south end of the belt of anomalously slow upper mantle seismic velocities adjacent to the (now) Afar depression at the (now) north end of the East African Rift system (fig. 14). This is consistent with these features collectively reflecting a formerly continuous structure, such as an arch in the base of the sub-continental lithosphere of east Africa and Arabia. Ebinger and Sleep (1998) recognized that because of substantial relief on the base of the Africa Plate, upwelling plume material could be channelized as it encountered and spread buoyantly beneath the lithosphere, producing belts of intraplate magmatism not obviously related to crustal terranes, active tectonics, or plate boundaries. This may have been the case for the Arabian harrat belt with portions of the Afar mantle plume, or adjacent ambient asthenosphere prompted into motion by the plume, spreading preferentially beneath a preexisting arch in the base of the lithosphere (Sisson and others, 2023b). Shear-wave speeds for the region are anisotropic with fast directions oriented generally north-south to about 20° west of north similar to the orientation of the harrats and the low-velocity belt in the upper mantle (Hansen and others, 2006; Chen and others, 2015); this fast direction can be interpreted as the direction of mantle flow. That the Red Sea did not rift along that belt may result from the Red Sea's orientation being approximately perpendicular to the direction of "slab pull" in the early Miocene (Reilinger and others, 2015) with the Red Sea effectively being a product of passive rifting.

The opening of the Red Sea and Gulf of Aden would have severed any formerly continuous arch in the base of the continental lithosphere, interrupting simple channelized flow from the Afar mantle plume; yet, harrat volcanism continued on the Arabia Plate possibly owing to at least two processes. Elkins-Tanton (2005) proposed a feedback mechanism wherein magmas produced by localized mantle upwelling solidify as eclogite upon intruding the base of the sub-continental lithosphere, increasing the density of the intruded region and fostering its foundering. As foundering takes place, asthenosphere upwells to replace the masses of sinking lithosphere, and as it does so, the upwelling asthenosphere undergoes decompression melting; those melts then intrude the deep lithosphere and also solidify as eclogites, prompting further foundering, and thereby continuing the process. Once commenced, the phenomenon might erode some distance up through the mantle lithosphere in a localized region, with associated continued magmatism, although the long-term persistence of the process has not been assessed by modeling. Alternatively, and independent of plumes, arches in the base of the sub-continental lithosphere exist for some reason, the simplest being that those areas are hotter than is typical for the terrane's age, as would be so if they are situated above persistent upwelling zones of the convecting ambient asthenosphere. Arrival of a plume might then accentuate upwelling already established beneath the thin lithosphere regions.

Harrat magmatism is a member of a cascade of phenomena that affected the Arabia Plate commencing in the Oligocene but accelerating in the Miocene. These include

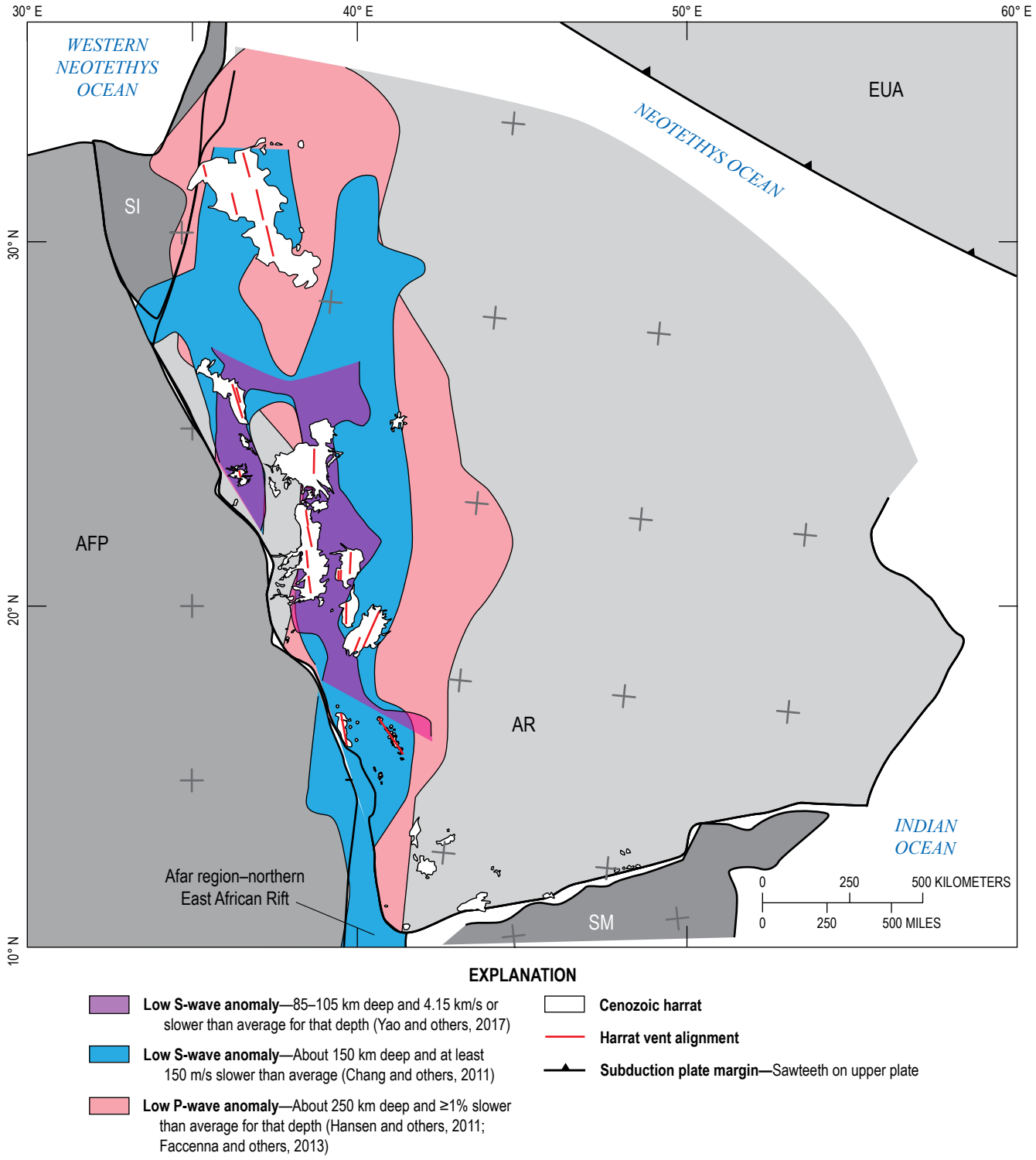

Figure 14. Schematic tectonic reconstruction of part of northeastern Africa, Arabia, and Eurasia showing the Red Sea and Gulfs of Aden, Suez, and Aqaba (see fig. 1 for locations) closed by holding the Africa Plate (AFP) fixed and translating and rotating the Arabia Plate (AR), Somali block (SM), and Sinai (SI) block to match opposing shorelines. Also shown are schematic locations of the Eurasia Plate (EUA) and its subduction zone, as well as flanking ocean basins. Note that the northeast edge of the Arabia Plate has been consumed by subduction beneath the Eurasia Plate, so its shape and extent are unknown. Translated and rotated within the Arabia Plate are its present-day harrats and their vent alignments, along with approximate areas of anomalously reduced velocities of shear waves (S-waves) and compression waves (P-waves). Black plus symbols, latitude and longitude ticks and values represent present-day (nonrotated) geographic locations, in 5° increments (using a Mercator projection) referenced to a fixed Africa Plate; gray plus symbols represent geographic locations that are translated and rotated, referenced to rotated lithospheric blocks. Figure modified from Sisson and others (2023b). km, kilometer; km/s, kilometer per second; m/s, meter per second.

(1) the opening of the Red Sea and Gulf of Aden leading to organized seafloor-spreading magmatism, (2) the uplift of the Arabian Shield from near sea level to its high elevations with associated outward tilting of the Arabian Platform sedimentary sequence and creation of the Great Escarpment, and (3) the severance of the Arabia Plate from the Sinai block along the Gulf of Aqaba-Dead Sea Transform fault system. The confluence of these events across a region much broader than the harrat belt points to a regional weakening of the Arabia Plate, with its widespread, coherent uplift consistent with loss of mantle lithosphere across a region more extensive than the zone of notably reduced seismic velocities. Potentially, arrival of the Afar mantle plume, or of associated smaller plumes to its north, stimulated asthenospheric convection sufficient to thin and weaken the continental plate from below to the point of its failure across distances of thousands of kilometers (Calvert and Sisson, 2023).

References Cited

Agard, P., Omrani, J., Jolivet, L., Whitechurch, H., Vrielynck, B., Spakman, W., Monié, P., Meyer, B., and Wortel, R., 2011, Zagros orogeny—A subduction-dominated process: Geological Magazine, v. 148, nos. 5–6, p. 692–725, https://doi.org/10.1017/S001675681100046X.

Al-Amri, A.M., Fnais, M.S., Abdel-Rahman, K., Mogren, S., and Al-Dabbagh, M., 2012, Geochronological dating and stratigraphic sequence of Harrat Lunayyir, NW Saudi Arabia: International Journal of Physical Sciences, v. 7, no. 20, p. 2791–2805, https://doi.org/10.5897/IJPS12.178.

Al-Onaizan, A.S., Al-Sheri, M.S., Hafez, K.H.A., and Al-Hussein, A.A.M., 2017, Volcanic fields in the Kingdom of Saudi Arabia: Jiddah, Saudi Arabia, Saudi Geological Survey, 570 p. [In Arabic.]

Altherr, R., Mertz-Kraus, R., Volker, F., Kreuzer, H., Henjes-Kunst, F., and Lange, U., 2019, Geodynamic setting of Upper Miocene to Quaternary alkaline basalts from Harrat al 'Uwayrid (NW Saudi Arabia)—Constraints from K-Ar dating, chemical and Sr-Nd-Pb isotope compositions, and petrological modeling: Lithos, v. 330–331, p. 120–138, https://doi.org/10.1016/j.lithos.2019.02.007.

Artemieva, I.M., 2006, Global 1°′1° thermal model TC1 for the continental lithosphere—Implications for lithosphere secular evolution: Tectonophysics, v. 416, nos. 1–4, p. 245–277, https://doi.org/10.1016/j.tecto.2005.11.022.

Baker, B.H., 1970, The structural pattern of the Afro-Arabian rift system in relation to plate tectonics: Philosophical Transactions of the Royal Society of London, Series A, Mathematical and Physical Sciences, v. 267, p. 383–391, https://www.jstor.org/stable/73628. https://doi.org/10.1098/rsta.1970.0043

Baker, J., Snee, L., and Menzies, M., 1996, A brief Oligocene period of flood volcanism in Yemen—Implications for the duration and rate of continental flood volcanism at the Afro–Arabian triple junction: Earth and Planetary Science Letters, v. 138, nos. 1–4, p. 39–55, https://doi.org/10.1016/0012-821X(95)00229-6.

Ball, P.W., Roberts, G.G., Mark, D.F., Barfod, D.N., White, N.J., Lodhia, B.H., Nahdi, M.M., and Garni, S., 2023, Geochemical and geochronological analysis of Harat Rahat, Saudi Arabia—An example of plume related intraplate magmatism: Lithos, v. 446–447, 17 p., https://doi.org/10.1016/j.lithos.2023.107112.

Bedrosian, P.A., Peacock, J.R., Dahry, M., Sharif, A., Feucht, D.W., and Zahran, H.M., 2019, Crustal magmatism and anisotropy beneath the Arabian Shield—A cautionary tale: Journal of Geophysical Research Solid Earth, v. 124, no. 10, p. 10153–10179, https://doi.org/10.1029/2019JB017903.

Bender, F., 1975, Geology of the Arabian Peninsula, Jordan: U.S. Geological Survey Professional Paper 560–I, 36-p. pamphlet, 3 pl., https://doi.org/10.3133/pp560I.

Blanchette, A.R., Klemperer, S.L., Mooney, W.D., and Zahran, H.M., 2018, Two-stage Red Sea rifting inferred from mantle earthquakes in Neoproterozoic lithosphere: Earth and Planetary Science Letters, v. 497, p. 92–101, https://doi.org/10.1016/j.epsl.2018.05.048.

Bohannon, R.G., 1986, Tectonic configuration of the western Arabian continental margin, southern Red Sea: Tectonics, v. 5, no. 4, p. 477–499, https://doi.org/10.1029/TC005i004p00477.

Bohannon, R.G., Naeser, C.W., Schmidt, D.L., and Zimmermann, R.A., 1989, The timing of uplift, volcanism, and rifting peripheral to the Red Sea—A case for passive rifting?: Journal of Geophysical Research Solid Earth, v. 94, no. B2, p. 1683–1701, https://doi.org/10.1029/JB094iB02p01683.

Bosworth, W., 2015, Geological evolution of the Red Sea—Historical background, review, and synthesis, *in* Rasul, N.M.A., and Stewart, I.C.F., eds., The Red Sea: Berlin, Springer-Verlag, p. 45–78, https://doi.org/10.1007/978-3-662-45201-1_3.

Bosworth, W., Huchon, P., and McClay, K., 2005, The Red Sea and Gulf of Aden basins: Journal of African Earth Science, v. 43, nos. 1–3, p. 334–378, https://doi.org/10.1016/j.jafrearsci.2005.07.020.

Bosworth, W., and Stockli, D.F., 2016, Early magmatism in the greater Red Sea rift—Timing and significance: Canadian Journal of Earth Sciences, v. 53, p. 1158–1176, https://doi.org/10.1139/cjes-2016-0019.

Brenna, M., Pontesilli, A., Mollo, S., Masotta, M., Cronin, S.J., Smith, I.E.M., Moufti, M.R.H., and Scarlato, P., 2019, Intra-eruptive trachyte-phonolite transition—Natural evidence and experimental constraints on the role of crystal mushes: American Mineralogist, v. 104, no. 12, p. 1750–1764, https://doi.org/10.2138/am-2019-6963.

Brown, G.F., Schmidt, D.L., and Huffman, A.C., Jr., 1989, Geology of the Arabian Peninsula—Shield area of western Saudi Arabia: U.S. Geological Survey Professional Paper 560–A, 188-p. pamphlet, 4 pl., https://doi.org/10.3133/pp560A.

Burke, K., and Dewey, J.F., 1973, Plume-generated triple junctions—Key indicators in applying plate tectonics to old rocks: Journal of Geology, v. 81, no. 4, p. 406–433, https://doi.org/10.1086/627882.

Calvert, A.T., and Sisson, T.W., 2023, Cenozoic tectonics of the western Arabia Plate related to harrat magmatism near Al Madīnah, Kingdom of Saudi Arabia, chap. B *of* Sisson, T.W., Calvert, A.T., and Mooney, W.D., eds., Active volcanism on the Arabian Shield—Geology, volcanology, and geophysics of northern Harrat Rahat and vicinity, Kingdom of Saudi Arabia: U.S. Geological Survey Professional Paper 1862 [also released as Saudi Geological Survey Special Report SGS–SP–2021–1], 29 p., https://doi.org/10.3133/pp1862B.

Camp, V.E., Hooper, P.R., Roobol, J.M., and White, D.L., 1987, The Madinah eruption, Saudi Arabia—Magma mixing and simultaneous extrusion of three basaltic chemical types: Bulletin of Volcanology, v. 49, p. 489–508, https://doi.org/10.1007/BF01245475.

Camp, V.E., and Roobol, M.J., 1989, The Arabian continental alkali basalt province—Part I. Evolution of Harrat Rahat, Kingdom of Saudi Arabia: Geological Society of America Bulletin, v. 101, no. 1, p. 71–95, https://doi.org/10.1130/0016-7606(1989)101<0071:TACABP>2.3.CO;2.

Camp, V.E., and Roobol, M.J., 1991a, Geologic map of the Cenozoic lava field of Harrat Rahat, Kingdom of Saudi Arabia: Saudi Arabian Ministry of Petroleum and Mineral Resources Geoscience Map GM–123, 37-p. pamphlet, scale 1:250,000.

Camp, V.E., and Roobol, M.J., 1991b, Comment on "Topographic and volcanic asymmetry around the Red Sea—Constraints on rift models" by T.H. Dixon, E.R. Ivins, and J.F. Brenda: Tectonics, v. 10, no. 3, p. 649–652, https://doi.org/10.1029/91TC00057.

Camp, V.E., and Roobol, M.J., 1992, Upwelling asthenosphere beneath western Arabia and its regional implications: Journal of Geophysical Research Solid Earth, v. 97, no. B11, p. 15255–15271, https://doi.org/10.1029/92JB00943.

Camp, V.E., Roobol, M.J., and Hooper, P.R., 1991, The Arabian continental alkali basalt province—Part II. Evolution of Harrats Khaybar, Ithnayn, and Kura, Kingdom of Saudi Arabia: Geological Society of America Bulletin, v. 103, no. 3, p. 363–391, https://doi.org/10.1130/0016-7606(1991)103<0363:TACABP>2.3.CO;2.

Camp, V.E., Roobol, M.J., and Hooper, P.R., 1992, The Arabian continental alkali basalt province—Part II. Evolution of Harrat Kishb, Kingdom of Saudi Arabia: Geological Society of America Bulletin, v. 104, no. 4, p. 379–396, https://doi.org/10.1130/0016-7606(1992)104<0379:TACABP>2.3.CO;2.

Champion, D.E., Downs, D.T., Stelten, M.E., Robinson, J.E., Sisson, T.W., Shawali, J., Hassan, K., and Zahran, H.M., 2023, Paleomagnetism of the Harrat Rahat volcanic field, Kingdom of Saudi Arabia—Geologic unit correlation and geomagnetic cryptochron identifications, chap. H *of* Sisson, T.W., Calvert, A.T., and Mooney, W.D., eds., Active volcanism on the Arabian Shield—Geology, volcanology, and geophysics of northern Harrat Rahat and vicinity, Kingdom of Saudi Arabia: U.S. Geological Survey Professional Paper 1862 [also released as Saudi Geological Survey Special Report SGS–SP–2021–1], 31 p., https://doi.org/10.3133/pp1862H.

Chang, S.-J., Merino, M., Van der Lee, S., Stein, S., and Stein, C.A., 2011, Mantle flow beneath Arabia offset from opening of the Red Sea: Geophysical Research Letters, v. 38, no. 4, 5 p., https://doi.org/10.1029/2010GL045852.

Chen, S., Mooney, W.D., Suzuki, J., Zahran, H.M., and El-Hadidy, S.Y., 2015, New measurements of shear-wave splitting in Saudi Arabia [abs.], *in* American Geophysical Union 48th Annual Fall Meeting 2015, San Francisco, California, December 14–18, 2015, Abstracts: American Geophysical Union, abstract T51G-3022. [Available at https://agu.confex.com/agu/fm15/meetingapp.cgi/Paper/76228.]

Civilini, F., Mooney, W.D., Savage, M.K., Townend, J., and Zahran, H., 2019, Crustal imaging of northern Harrat Rahat, Saudi Arabia, from ambient noise tomography: Geophysical Journal International, v. 219, no. 3, p. 1532–1549, https://doi.org/10.1093/gji/ggz380.

Coleman, R.G., 1974, Geologic background of the Red Sea, *in* Whitmarsh, R.B., Weser, O.E., and Ross, D.A., eds., Deep Sea Drilling Project covering Leg 23 of the cruises of the drilling vessel *Glomar Challenger* Colombo, Ceylon to Djibouti, F.T.A.I., March–May 1972, sites 219–230: Initial Reports of the Deep Sea Drilling Project, chap. 21 *of* v. XXIII, p. 813–819. [Available at http://doi.org/10.2973/dsdp.proc.23.121.1974.]

Coleman, R.G., 1993, Geologic evolution of the Red Sea: Oxford University Press, Oxford Monographs on Geology and Geophysics, no. 24, 186 p.

Coleman, R.G., Gregory, R.T., and Brown, G.F., 1983, Cenozoic volcanic rocks of Saudi Arabia: U.S. Geological Survey Open-File Report 83–788, 82 p., 1 pl., https://doi.org/10.3133/ofr83788.

Dietterich, H.R., Downs, D.T., and Stelten, M.E., 2023, Lava flow emplacement in Harrat Rahat with implications for eruptions in mafic volcanic fields, chap. E *of* Sisson, T.W., Calvert, A.T., and Mooney, W.D., eds., Active volcanism on the Arabian Shield—Geology, volcanology, and geophysics of northern Harrat Rahat and vicinity, Kingdom of Saudi Arabia: U.S. Geological Survey Professional Paper 1862 [also released as Saudi Geological Survey Special Report SGS–SP–2021–1], 49 p., https://doi.org/10.3133/pp1862E.

Dietterich, H.R., Downs, D.T., Stelten, M.E., and Zahran, H., 2018, Reconstructing lava flow emplacement histories with rheological and morphological analysis—The Harrat Rahat volcanic field, Kingdom of Saudi Arabia: Bulletin of Volcanology, v. 80, article 85, https://doi.org/10.1007/s00445-018-1259-4.

Downs, D.T., 2019, Major- and trace-element chemical analyses of rocks from the northern Harrat Rahat volcanic field and surrounding area, Kingdom of Saudi Arabia: U.S. Geological Survey data release, https://doi.org/10.5066/P91HL91C.

Downs, D.T., Robinson, J.E., Stelten, M.E., Champion, D.E., Dietterich, H.R., Sisson, T.W., Zahran, H., Hassan, K., and Shawali, J., 2019, Geologic map of the northern Harrat Rahat volcanic field, Kingdom of Saudi Arabia: U.S. Geological Survey Scientific Investigations Map 3428 [also released as Saudi Geological Survey Special Report SGS–SP–2019–2], 64-p. pamphlet, 4 sheets, scales 1:75,000 and 1:25,000, https://doi.org/10.3133/sim3428.

Downs, D.T., Stelten, M.E., Champion, D.E., Dietterich, H.R., Nawab, Z., Zahran, H., Hassan, K., and Shawali, J., 2018, Volcanic history of the northernmost part of the Harrat Rahat volcanic field, Kingdom of Saudi Arabia: Geosphere, v. 14, no. 3, p. 1253–1282, https://doi.org/10.1130/GES01625.1.

Downs, D.T., Stelten, M.E., Dietterich, H.R., Champion, D.E., Mahood, G.A., Sisson, T.W., Calvert, A.T., and Shawali, J., 2023, Explosive trachyte eruptions from the Al Efairia volcanic center in northern Harrat Rahat, Kingdom of Saudi Arabia, chap. G *of* Sisson, T.W., Calvert, A.T., and Mooney, W.D., eds., Active volcanism on the Arabian Shield—Geology, volcanology, and geophysics of northern Harrat Rahat and vicinity, Kingdom of Saudi Arabia: U.S. Geological Survey Professional Paper 1862 [also released as Saudi Geological Survey Special Report SGS–SP–2021–1], 14 p., https://doi.org/10.3133/pp1862G.

Ebinger, C.J., and Sleep, N.H., 1998, Cenozoic magmatism throughout east Africa resulting from a single plume: Nature, v. 395, p. 788–791, https://doi.org/10.1038/27417.

Elkins-Tanton, L.T., 2005, Continental magmatism caused by lithospheric delamination, *in* Foulger, G.R., Natland, J.H., Presnall, D.C., and Anderson, D.L., eds., Plates, plumes, and paradigms: Geological Society of America Special Paper 388, p. 449–461, https://doi.org/10.1130/0-8137-2388-4.449.

Ewart, A., Chappell, B.W., and Menzies, M.A., 1988, An overview of the geochemical and isotopic characteristics of the Eastern Australian Cainozoic Volcanic Provinces: Journal of Petrology Special Volume, no. 1, p. 225–273, https://doi.org/10.1093/petrology/Special_Volume.1.225.

Faccenna, C., Becker, T.W., Jolivet, L., and Keskin, M., 2013, Mantle convection in the Middle East—Reconciling Afar upwelling, Arabia indentation and Aegean trench rollback: Earth and Planetary Science Letters, v. 375, p. 254–269, https://doi.org/10.1016/j.epsl.2013.05.043.

Faccenna, C., Glišović, P., Forte, A., Becker, T.W., Garzanti, E., Sembroni, A., and Gvirtzman, Z., 2019, Role of dynamic topography in sustaining the Nile River over 30 million years: Nature Geoscience, v. 12, p. 1012–1017, https://doi.org/10.1038/s41561-019-0472-x.

Gale, A., Dalton, C.A., Langmuir, C.H., Su, Y., and Schilling, J.-G., 2013, The mean composition of ocean ridge basalts: Geochemistry, Geophysics, Geosystems, v. 14, no. 3, p. 489–518, https://doi.org/10.1029/2012GC004334.

Geukens, F., 1966, Geology of the Arabian Peninsula, Yemen: U.S. Geological Survey Professional Paper 560–B, 23 p., https://doi.org/10.3133/pp560B.

Groucutt, H.S., Breeze, P.S., Guagnin, M., Stewart, M., Drake, N., Shipton, C., Zahrani, B., Omarfi, A.A., Alsharekh, A.M., and Petraglia, M.D., 2020, Monumental landscapes of the Holocene humid period in Northern Arabia—The mustatil phenomenon: Holocene, v. 30, no. 12, p. 1767–1779, https://doi.org/10.1177/0959683620950449.

Hacker, B.R., Kelemen, P.B., and Behn, M.D., 2015, Continental lower crust: Annual Reviews of Earth and Planetary Sciences, v. 43, p. 167–205, https://doi.org/10.1146/annurev-earth-050212-124117.

Hansen, S.E., Nyblade, A.A., and Benoit, M.H., 2012, Mantle structure beneath Africa and Arabia from adaptively parameterized P-wave tomography—Implications for the origin of Cenozoic Afro-Arabian tectonism: Earth and Planetary Science Letters, v. 319–320, p. 23–34, https://doi.org/10.1016/j.epsl.2011.12.023.

Hansen, S.E., Rodgers, A.J., Schwartz, S.Y., and Al-Amri, A.M.S., 2007, Imaging ruptured lithosphere beneath the Red Sea and Arabian Peninsula: Earth and Planetary Science Letters, v. 259, p. 256–265, https://doi.org/10.1016/j.epsl.2007.04.035.

Hansen, S., Schwartz, S., Al-Amri, A., and Rodgers, A., 2006, Combined plate motion and density-driven flow in the asthenosphere beneath Saudi Arabia—Evidence from shear-wave splitting and seismic anisotropy: Geology, v. 34, no. 10, p. 869–872, https://doi.org/10.1130/G22713.1.

Hart, S.R., 1984, A large scale isotope anomaly in the Southern Hemisphere mantle: Nature, v. 309, p. 753–757, https://doi.org/10.1038/309753a0.

Ilani, S., Harlavan, Y., Tarawneh, K., Rabba, I., Weinberger, R., Ibrahim, K., Peltz, S., and Steinitz, G., 2001, New K-Ar ages of basalts from the Harrat Ash Shaam volcanic field in Jordan—Implications for the span and duration of the upper mantle upwelling beneath the western Arabian plate: Geology, v. 29, no. 2, p. 171–174, https://doi.org/10.1130/0091-7613(2001)029<0171:NKAAOB>2.0.CO;2.

Irvine, T.N., and Baragar, W.R.A., 1971, A guide to the chemical classification of common volcanic rocks: Canadian Journal of Earth Sciences, v. 8, no. 5, p. 523–548, https://doi.org/10.1139/e71-055.

Johnson, P.R., and Kattan, F.H., 2012, The geology of the Saudi Arabian Shield: Jiddah, Saudi Arabia, Saudi Geological Survey, 479 p.

Kawabata, E., Cronin, S.J., Bebbington, M.S., Moufti, M.R.H., El-Masry, N., and Wang, T., 2015, Identifying multiple eruption phases from a compound tephra blanket—An example of the AD1256 Al-Madinah eruption, Saudi Arabia: Bulletin of Volcanology, v. 77, article 6, p. 1–13, https://doi.org/10.1007/s00445-014-0890-y.

Kereszturi, G., Németh, K., Moufti, M.R., Cappello, A., Murcia, H., Ganci, G., Del Negro, C., Procter, J., and Zahran, H.M.A., 2016, Emplacement conditions of the 1256AD Al-Madinah lava flow field in Harrat Rahat, Kingdom of Saudi Arabia—Insights from surface morphology and lava flow simulations: Journal of Volcanology and Geothermal Research, v. 309, p. 14–30, https://doi.org/10.1016/j.jvolgeores.2015.11.002.

Lamare, P., 1924, L'Arabie Heureuse—Le Yémen [Arabia the felicitous—Yemen]: Géographie, v. 42, no. 1, p. 1–23. [Available at https://gallica.bnf.fr/ark:/12148/bpt6k377784/f11.item. In French.]

Lamare, P., 1930, Les manifestations volcaniques post-Crétacées de la Mer Rouge et des pays limitrophes [Post-Cretaceous volcanic manifestations of the Red Sea and surrounding areas], *in* Teilhard de Chardin, P., Lamare, P., Dreyfuss, M., Lacroix, A., and Basse, E., Études Géologiques en Éthiopie, Somalie et Arabie Méridionale [Geological studies in Ethiopia, Somalia and southern Arabia]: Mémoires de la Société Géologique de France, Nouvelle Série, v. VI, Mémoire 14, p. 21–48. [Available at https://babel.hathitrust.org/cgi/pt?id=uiug.30112026649258&seq=13. In French.]

Langenheim, V.E., Ritzinger, B.T., Zahran, H., Shareef, A., and Al-dahri, M., 2019, Crustal structure of the northern Harrat Rahat volcanic field (Saudi Arabia) from gravity and aeromagnetic data: Tectonophysics, v. 750, p. 9–21, https://doi.org/10.1016/j.tecto.2018.11.005.

Langenheim, V.E., Ritzinger, B.T., Zahran, H.M., Shareef, A., and Al-Dhahry, M.K., 2023, Depth to basement and crustal structure of the northern Harrat Rahat volcanic field, Kingdom of Saudi Arabia, from gravity and aeromagnetic data, chap. K *of* Sisson, T.W., Calvert, A.T., and Mooney, W.D., eds., Active volcanism on the Arabian Shield—Geology, volcanology, and geophysics of northern Harrat Rahat and vicinity, Kingdom of Saudi Arabia: U.S. Geological Survey Professional Paper 1862 [also released as Saudi Geological Survey Special Report SGS–SP–2021–1], 18 p., https://doi.org/10.3133/pp1862K.

Lartet, L., 1869, Essai sur la géologie de la Palestine et des contrées avoisinantes, telles que L'Egypte el L'Arabie, comprenant les observations recueillies dans le cours de l'expédition du Duc de Luynes a la Mer Morte [Essay on the geology of Palestine and neighboring countries, such as Egypt and Arabia, including observations collected during the expedition of the Duke of Luynes to the Dead Sea]: Paris, Annales des Sciences Géologiques, Victor Masson et Fils, v. 1, p. 5–116. [In French.]

Le Bas, M.J., and Streckeisen, A.L., 1991, The IUGS systematics of igneous rocks: Journal of the Geological Society, v. 148, p. 825–833, https://doi.org/10.1144/gsjgs.148.5.0825.

Lindsay, J.M., and Moufti, M.R., 2014, Assessing volcanic risk in Saudi Arabia: Eos, v. 95, no. 31, p. 277–278, https://doi.org/10.1002/2014EO310002.

MacDonald, G.A., and Katsura, T., 1964, Chemical composition of Hawaiian lavas: Journal of Petrology, v. 5, no. 1, p. 82–133, https://doi.org/10.1093/petrology/5.1.82.

Madden, C.T., Naqvi, I.M., Whitmore, F.E., Jr., Schmidt, D.L., Langston, W., and Wood, R.C., 1980, Paleocene vertebrates from coastal deposits in the Harrat Hadan area, At Taif region, Kingdom of Saudi Arabia: U.S. Geological Survey Open File Report 80–227, 29 p., 1 pl., https://doi.org/10.3133/ofr80227.

McGuire, A.V., and Bohannon, R.G., 1989, Timing of mantle upwelling—Evidence for a passive rift origin for the Red Sea: Journal of Geophysical Research Solid Earth, v. 94, no. B2, p. 1677–1682, https://doi.org/10.1029/JB094iB02p01677.

McKenzie, D.P., Davies, D., and Molnar, P., 1970, Plate tectonics of the Red Sea and East Africa: Nature, v. 226, p. 243–248, https://doi.org/10.1038/226243a0.

McQuarrie, N., and van Hinsbergen, D.J.J., 2013, Retrodeforming the Arabia-Eurasia collision zone—Age of collision versus magnitude of continental subduction: Geology, v. 41, no. 3, p. 315–318, https://doi.org/10.1130/G33591.1.

McQuarrie, N., Stock, J.M., Verdel, C., and Wernicke, B.P., 2003, Cenozoic evolution of Neotethys and implications for the causes of plate motions: Geophysical Research Letters, v. 30, no. 20, article 2036, 4 p., https://doi.org/10.1029/2003GL017992.

Meissner, C.R., Jr., Griffin, M.B., Riddler, G.P., Van Eck, M., Aspinall, N.C., Farasani, A.M., and Dini, S.M., 1990, Preliminary geologic map of the Wadi As Sirhan Quadrangle, sheet 30C, Kingdom of Saudi Arabia: U.S. Geological Survey Open-File Report 90–263, 33 p., 2 pls., https://doi.org/10.3133/ofr90263.

Menzies, M., Baker, J., Chazot, G., and Al'Kadasi, M., 1997, Evolution of the Red Sea volcanic margin, western Yemen, *in* Mahoney, J.J., and Coffin, M.F., eds., Large igneous provinces, continental, oceanic, and planetary flood volcanism: American Geophysical Union Geophysical Monograph 100, p. 29–43, https://doi.org/10.1029/GM100p0029.

Minster, J.F., and Allègre, C.J., 1978, Systematic use of trace elements in igneous processes—III. Inverse problem of melting in volcanic suites: Contributions to Mineralogy and Petrology, v. 68, p. 37–52, https://doi.org/10.1007/BF00375445.

Minissale, A., Mattash, M.A., Vaselli, O., Tassi, F., Al-Ganad, I.N., Selmo, E., Shawki, N.M., Tedesco, D., Poreda, R., Ad-Dukhain, A.M., and Hazzae, M.K., 2007, Thermal springs, fumaroles and gas vents of continental Yemen—Their relation with active tectonics, regional hydrology and the country's geothermal potential: Applied Geochemistry, v. 22, p. 799–820, https://doi.org/10.1016/j.apgeochem.2006.11.009.

Moritz, B., 1923, Arabien—Studien zur physikalischen und historischen Geographie des Landes [Arabia—Studies in the physical and historical geography of the country]: Hannover, Germany, Heintz Lafaire, 133 p. [Available at https://babel.hathitrust.org/cgi/pt?id=wu.89098701725&seq=7. In German.]

Moufti, M.R.H., 1985, The geology of Harrat Al Madinah volcanic field Harrat Rahat, Saudi Arabia: Lancaster, United Kingdom, Lancaster University, Ph.D. dissertation, 2 vol., 476 p.

Moufti, M.R., and Németh, K., 2016, Geoheritage of volcanic harrats in Saudi Arabia: Switzerland, Springer, 194 p. https://doi.org/10.1007/978-3-319-33015-0

Murcia, H., Németh, K., El-Masry, N.N., Lindsay, J.M., Moufti, M.R.H, Wameyo, P., Cronin, S.J., Smith, I.E.M., and Kereszturi, G., 2015, The Al-Du'aythah volcanic cones, Al-Madinah City—Implications for volcanic hazards in northern Harrat Rahat, Kingdom of Saudi Arabia: Bulletin of Volcanology, v. 77, article 54, p. 1–19, https://doi.org/10.1007/s00445-015-0936-9.

Neumann van Padang, M., 1963, Catalogue of the active volcanoes and solfatara fields of Arabia and the Indian Ocean, Part XVI *of* Catalogue of the active volcanoes of the World: Rome, International Association of Volcanology, 64 p.

O'Neill, H.S.C., 2016, The smoothness and shapes of chondrite-normalized rare earth element patterns in basalts: Journal of Petrology, v. 57, no. 8, p. 1463–1508, https://doi.org/10.1093/petrology/egw047.

Pallister, J.S., McCausland, W.D., Jónsson, S., Lu, Z., Zahran, H.M., El Hadidy, S., Aburukbah, A., Stewart, I.C.F., Lundgren, P.R., White, R.A., and Moufti, M.R.H., 2010, Broad accommodation of rift-related extension recorded by dyke intrusion in Saudi Arabia: Nature Geoscience, v. 3, p. 705–712, https://doi.org/10.1038/ngeo966.

Peacock, J.R., Bedrosian, P.A., Al-Dhahry, M.K., Shareef, A., Feucht, D.W., Taylor, C.D., Bloss, B., and Zahran, H.M., 2023, Magnetotelluric investigation of northern Harrat Rahat, Kingdom of Saudi Arabia, chap. L *of* Sisson, T.W., Calvert, A.T., and Mooney, W.D., eds., Active volcanism on the Arabian Shield—Geology, volcanology, and geophysics of northern Harrat Rahat and vicinity, Kingdom of Saudi Arabia: U.S. Geological Survey Professional Paper 1862 [also released as Saudi Geological Survey Special Report SGS–SP–2021–1], 111 p., https://doi.org/10.3133/pp1862L.

Pellaton, C., 1981, Geologic map of the Al Madinah quadrangle, sheet 24D, Kingdom of Saudi Arabia: Saudi Arabian Deputy Ministry for Mineral Resources Geologic Map GM–52C, 19-p. pamphlet, 1 sheet, scale 1:250,000.

Ponikarov, V., and Mikhailov, I., 1986, Geological map of Syria (2d ed.): Syrian Arab Republic, Ministry of Petroleum and Mineral Resources, 4 sheets, scale 1:1,000,000.

Powers, R.W., Ramirez, L.F., Redmond, C.D., and Elberg, E.L., Jr., 1966, Sedimentary geology of Saudi Arabia, *in* Geology of the Arabian Peninsula: U.S. Geological Survey Professional Paper 560–D, 147 p., https://doi.org/10.3133/pp560D.

Reilinger, R., McClusky, S., and ArRajehi, A., 2015, Geodetic constraints on the geodynamic evolution of the Red Sea, *in* Rasul, N.M.A., and Stewart, I.C.F., eds., The Red Sea: Berlin, Springer-Verlag, Springer Earth System Sciences, p. 135–149.

Richard, J.J., and Neumann van Padang, M., 1957, Catalogue of the active volcanoes and solfatara fields of Africa and the Red Sea, Part IV *of* Catalogue of the active volcanoes of the world including solfatara fields: Rome, International Association of Volcanology, 118 p.

Robinson, J.E, and Downs, D.T., 2023, Overview of the Cenozoic geology of the northern Harrat Rahat volcanic field, Kingdom of Saudi Arabia, chap. R *of* Sisson, T.W., Calvert, A.T., and Mooney, W.D., eds., Active volcanism on the Arabian Shield—Geology, volcanology, and geophysics of northern Harrat Rahat and vicinity, Kingdom of Saudi Arabia: U.S. Geological Survey Professional Paper 1862 [also released as Saudi Geological Survey Special Report SGS–SP–2021–1], 20 p., 1 pl., scale 1:100,000, https://doi.org/10.3133/pp1862R.

Rolandone, F., Lucazeau, F., Leroy, S., Mareschal, J.-C., Jorand, J., Goutorbe, B., and Bouquerel, H., 2013, New heat flow measurements in Oman and the thermal state of the Arabian Shield and Platform: Tectonophysics, v. 589, p. 77–89, https://doi.org/10.1016/j.tecto.2012.12.034.

Roobol, J.M., and Camp, V.E., 1991a, Geologic map of the Cenozoic lava fields of Harrats Khaybar, Ithnayn, and Kura, Kingdom of Saudi Arabia: Saudi Arabian Ministry of Petroleum and Mineral Resources Geoscience Map GM–131, 40-p. pamphlet, 1 sheet, 1:250,000 scale.

Roobol, J.M., and Camp, V.E., 1991b, Geologic map of the Cenozoic lava fields of Harrat Kishb, Kingdom of Saudi Arabia: Saudi Arabian Ministry of Petroleum and Mineral Resources Geoscience Map GM–132, 34-p. pamphlet, 1 sheet, 1:250,000 scale.

Runge, M.G., Bebbington, M.S., Cronin, S.J., Lindsay, J.M., Kenedi, C.L., and Moufti, M.R.H., 2014, Vents to events—Determining an eruption event record from volcanic vent structures for the Harrat Rahat, Saudi Arabia: Bulletin of Volcanology, v. 76, article 804, p. 1–16, https://doi.org/10.1007/s00445-014-0804-z.

Ryan, W.B.F., Carbotte, S.M., Coplan, J.O., O'Hara, S., Melkonian, A., Arko, R., Weissel, R.A., Ferrini, V., Goodwillie, A., Nitsche, F., Bonczkowski, J., and Zemsky, R., 2009, Global multi-resolution topography synthesis: Geochemistry, Geophysics, Geosystems, v. 10, no. 3, article Q03014, https://doi.org/10.1029/2008GC002332.

Salters, V.J.M., Sachi-Kocher, A., Downs, D.T., Stelten, M.E., and Sisson, T.W., 2023, Isotopic and geochemical evidence for the sources of volcanism at Harrat Rahat, Kingdom of Saudi Arabia, chap. J *of* Sisson, T.W., Calvert, A.T., and Mooney, W.D., eds., Active volcanism on the Arabian Shield—Geology, volcanology, and geophysics of northern Harrat Rahat and vicinity, Kingdom of Saudi Arabia: U.S. Geological Survey Professional Paper 1862 [also released as Saudi Geological Survey Special Report SGS–SP–2021–1], 30 p., https://doi.org/10.3133/pp1862J.

Salters, V.J.M., and Stracke, A., 2004, Composition of the depleted mantle: Geochemistry, Geophysics, Geosystems, v. 5, no. 5, 27 p., https://doi.org/10.1029/2003GC000597.

Sarafian, E., Gaetani, G.A., Hauri, E.H., and Sarafian, A.R., 2017, Experimental constraints on the damp peridotite solidus and oceanic mantle potential temperature: Science, v. 355, no. 6328, p. 942–945, https://doi.org/10.1126/science.aaj2165.

Sebai, A., Zumbo, V., Féraud, G., Bertrand, H., Hassain, A.G., Giannérini, G., and Campredon, R., 1991, $^{40}Ar/^{39}Ar$ dating of alkaline and tholeiitic magmatism of Saudi Arabia related to the early Red Sea rifting: Earth and Planetary Science Letters, v. 104, nos. 2–4, p. 473–487, https://doi.org/10.1016/0012-821X(91)90223-5.

Sembroni, A., Faccenna, C., Becker, T.W., Molin, P., and Abebe, B., 2016, Long-term, deep-mantle support of the Ethiopia–Yemen Plateau: Tectonics, v. 35, no. 2, p. 469–488, https://doi.org/10.1002/2015TC004000.

Shanahan, T.M., McKay, N.P., Hugen, K.A., Overpeck, J.T., Otto-Bliesner, B., Heil, C.W., King, J., Scholz, C.A., and Peck, J., 2015, The time-transgressive termination of the African humid period: Nature Geoscience, v. 8, p. 140–144, https://doi.org/10.1038/ngeo2329.

Shea, J.J., Ezad, I.S., Foley, S.F., and Lanati, A.W., 2022, The Eastern Australian Volcanic Province, its primitive melts, constraints on melt sources and the influence of mantle metasomatism: Earth-Science Reviews, v. 233, article 104168, 23 p., https://doi.org/10.1016/j.earscirev.2022.104168.

Siebert, L., Simkin, T., and Kimberly, P., 2010, Volcanoes of the world (3d ed.): Berkeley, Calif., University of California Press, 551 p.

Sisson, T.W., Calvert, A.T., and Mooney, W.D., eds., 2023a, Active volcanism on the Arabian Shield—Geology, volcanology, and geophysics of northern Harrat Rahat and vicinity, Kingdom of Saudi Arabia: U.S. Geological Survey Professional Paper 1862 [also released as Saudi Geological Survey Special Report SGS–SP–2021–1], 610 p., https://doi.org/10.3133/pp1862.

Sisson, T.W., Downs, D.T., Calvert, A.T., Dietterich, H.R., Mahood, G.A., Salters, V.J.M., Stelten, M.E., and Shawali, J., 2023b, Mantle origin and crustal differentiation of basalts and hawaiites of northern Harrat Rahat, Kingdom of Saudi Arabia, chap. I *of* Sisson, T.W., Calvert, A.T., and Mooney, W.D., eds., Active volcanism on the Arabian Shield—Geology, volcanology, and geophysics of northern Harrat Rahat and vicinity, Kingdom of Saudi Arabia: U.S. Geological Survey Professional Paper 1862 [also released as Saudi Geological Survey Special Report SGS–SP–2021–1], 42 p., https://doi.org/10.3133/pp1862I.

Smith, J.W., 1980, Reconnaissance geologic map of the Wadi Mahani quadrangle sheet 22/40A Kingdom of Saudi Arabia: Saudi Arabian Deputy Ministry of Mineral Resources Geologic Map GM–35, scale 1:100,000, with text, 18 p.

Smith, J.W., 1982, Reconnaissance geologic map of the Wadi Hammah quadrangle sheet 22/40C Kingdom of Saudi Arabia: Saudi Arabian Deputy Ministry of Mineral Resources Geologic Map GM–65, scale 1:100,000, with text, 19 p.

Sneh, A., Bartov, Y., Weissbrod, T., and Rosensaft, M., 1998, Geological map of Israel: Israel Geological Survey, 4 sheets, scale 1:200,000. [Reprinted 2014. Available from the Geological Institute of Israel at https://www.gov.il/he/pages/israel-map-1-200k.]

Stelten, M.E., Downs, D.T., Champion, D.T., Dietterich, H.R., Calvert, A.T., Sisson, T.W., Mahood, G.A., and Zahran, H., 2020, The timing and compositional evolution of volcanism within northern Harrat Rahat, Kingdom of Saudi Arabia: Geological Society of America Bulletin, v. 132, nos. 7–8, p. 1381–1403, https://doi.org/10.1130/B35337.1.

Stelten, M.E., Downs, D.T., Dietterich, H.R., Calvert, A.T., Sisson, T.W., Mahood, G.A., and Zahran, H.M., 2023, Eruptive history of northern Harrat Rahat—Volume, timing, and composition of volcanism over the past 1.2 Ma, chap. D *of* Sisson, T.W., Calvert, A.T., and Mooney, W.D., eds., Active volcanism on the Arabian shield—Geology, volcanology, and geophysics of northern Harrat Rahat and vicinity, Kingdom of Saudi Arabia: U.S. Geological Survey Professional Paper 1862 [also released as Saudi Geological Survey Special Report SGS–SP–2021–1], 46 p., https://doi.org/10.3133/pp1862D.

Stelten, M.E., Downs, D.T., Dietterich, H.R., Mahood, G.A., Calvert, A.T., Sisson, T.W., Zahran, H., and Shawali, J., 2018, Timescales of magmatic differentiation from alkali basalt to trachyte within the Harrat Rahat volcanic field, Kingdom of Saudi Arabia: Contributions to Mineralogy and Petrology, v. 173, article 68, 17 p., https://doi.org/10.1007/s00410-018-1495-9.

Stern, R.J., and Johnson, P., 2010, Continental lithosphere of the Arabian plate—A geologic, petrologic, and geophysical synthesis: Earth-Science Reviews, v. 101, nos. 1–2, p. 29–67, https://doi.org/10.1016/j.earscirev.2010.01.002.

Sun, S.-s., and McDonough, W.F., 1989, Chemical and isotopic systematics of oceanic basalts—Implications for mantle composition and processes, *in* Saunders, A.D., and Norry, M.J., eds., Magmatism in the ocean basins, Leicester (UK), January 1987, Proceedings: Oxford, Blackwell Scientific Publications, Geological Society of London Special Publication 42, p. 313–345, https://doi.org/10.1144/GSL.SP.1989.042.01.19.

Swift, S.A., Uchupi, E., and Ross, D.A., 1998, Late Cenozoic geology of the central Persian (Arabian) Gulf from industry well data and seismic profiles: Woods Hole Oceanographic Institution Technical Memorandum WHOI–01–98, 75 p., accessed December 20, 2020, at https://hdl.handle.net/1912/1926.

Szymanski, E., Stockli, D.F., Johnson, P.R., and Hager, C., 2016, Thermochronometric evidence for diffuse extension and two-phase rifting within the central Arabian margin of the Red Sea Rift: Tectonics, v. 35, no. 12, p. 2863–2895, https://doi.org/10.1002/2016TC004336.

Torsvik, T.H., and Cocks, R.M., 2017, Earth history and palaeogeography: Cambridge, United Kingdom, Cambridge University Press, 317 p.

U.S. Geological Survey and Arabian American Oil Company, 1963, Geologic map of the Arabian Peninsula: U.S. Geological Survey Miscellaneous Geological Investigations Map I–270 A, 1 sheet, scale 1:2,000,000, https://doi.org/10.3133/i270A.

Walker, G.P.L., 1993, Basaltic-volcano systems, *in* Prichard, H.M., Alabaster, T., Harris, N.B.W., and Neary, C.R., eds., Magmatic processes and plate tectonics: London, Geological Society Special Publication 76, no. 1, p. 3–38, https://doi.org/10.1144/GSL.SP.1993.076.01.01.

Wegener, A., 1915, Die entstehung der kontinente und ozeane (1st ed.) [The origin of continents and oceans]: Braunschweig, Germany, Friedrich Vieweg & Sohn, 94 p. [In German.]

Wetzstein, J.G., 1860, Reisebericht über Hauran und die Trachonen nebst einem anhange über die Sabäischen denkmäler in Ostsyrien [Travel report about Hauran and the Trachonen with an appendix about the Sabbatean monuments in eastern Syria]: Berlin, Dietrich Reimer, 150 p., 1 map sheet, 1:400,000. [In German.]

Willett, W., Jenny, B., Isenberg, T. and Dragicevic, P., 2015, Lightweight relief shearing for enhanced terrain perception on interactive maps: Proceedings of the 33rd ACM Conference on Human Factors in Computing Systems (CHI 2015), April 2015, Seoul, South Korea, p. 3563–3572. https://doi.org/10.1145/2702123.2702172

Wissmann, H.von, Rathjens, C., and Kossmat, F., 1943, Beiträge zur tectonic Arabiens [Contributions to Arabian tectonics]: Geologische Rundschau, v. 33, p. 221–353, https://doi.org/10.1007/BF02200690. [In German.]

Workman, R.K., and Hart, S.R., 2005, Major and trace element composition of the depleted MORB mantle (DMM): Earth and Planetary Science Letters, v. 231, nos. 1–2, p. 53–72, https://doi.org/10.1016/j.epsl.2004.12.005.

Yao, Z., Mooney, W.D., Zahran, H.M., and Youseef, S.E-H., 2017, Upper mantle velocity structure beneath the Arabian shield from Rayleigh surface wave tomography and its implications: Journal of Geophysical Research Solid Earth, v. 122, no. 8, p. 6552–6568, https://doi.org/10.1002/2016JB013805.

Moffett Field Publishing Service Center, California
Approved for publication on August 5, 2024
Edited by Lisa Binder and Monica Erdman
Layout and design by Cory Hurd

ISSN 2330-7102 (online)
https://doi.org/10.3133/pp1890J